STRATIGRAPHIC, PETROGRAPHIC, AND SEDIMENTOLOGIC ANALYSIS OF UPPER CRETACEOUS DELTAIC SEDIMENTATION OF THE ADAVILLE FORMATION, KEMMERER COAL MINE AREA, SOUTHWESTERN WYOMING

A THESIS
SUBMITTED TO THE FACULTY OF THE GRADUATE SCHOOL OF THE
UNIVERSITY OF MINNESOTA
BY

CHAD ELLIOTT HEINZEL

IN PARTIAL FULFILLMENT OF THE REQUIREMENTS
FOR THE DEGREE OF
MASTER OF SCIENCE

February, 2000

Abstract

The Late Cretaceous Lazeart Member, the lower member of the Adaville Formation in southwestern Wyoming, has been interpreted as a wave-dominated deltaic complex. Studied sandstone outcrops include Crockers Point, Skull Point, and sandy layers within the Adaville Formation at the P&M Coal Mine near Kemmerer. The Adaville Formation, 620 m thick, consists of interbedded brownish shale, siltstone, sandstone layers, and coal seams. One coal bed exceeds 30 m in thickness. The average QmFLt ratio for the Adaville sandstones is 71:10:19; they are feldspathic sublitharenites. The average QmFLt ratio for the Lazeart sandstones is 58:10:32; they are classified as feldspathic lithic arenites.

Petrographic study revealed the presence of quartz overgrowths, vermicular kaolinite, partially dissolved K-feldspars, silica cement, and clay matrix undergoing various stages of diagenesis. The average porosities of the Adaville Formation and Lazeart Member are 6.3 and 12.6 percent, respectively. Primary porosity has been decreased by quartz overgrowths and vermicular kaolinite.

Two source areas contributed sediment to the Adaville Formation. The Idaho batholith shed metamorphic fragments, euhedral zircons, and K-feldspar - bearing plutonic fragments. In addition, Paleozoic sedimentary rocks thrust upward by the Absaroka and older faults contributed mud-siltstone fragments, rounded zircons, rounded tourmaline, and chert grains. Clastic debris from both source areas was transported along fluvial channels into a rapidly subsiding foreland basin adjacent to the Sevier Orogenic Belt. A regressive-transgressive epeiric seaway reworked sediments and placed morphologic constraints on the Lazeart wave-dominated delta.

TABLE OF CONTENTS

List of Figures

List of Tables

Acknowledgements

I dedicate this work to my grandfather, Donald O. Schwenker, and my family for their support and interest in my education. I am grateful for the advisement of those on my thesis committee - Dr. Richard Ojakangas, Dr. Charles Matsch, and Dr. Tom Johnson. I would like to thank the P&M Mining Company and especially Lynn Sessions for their cooperation with my field studies. I would like to thank Dr. Robert Hooper and University of Wisconsin-Eau Claire for use of their SEM. I also appreciate the help of Dr. Penelope Morton with XRD data gathering. Finally, I would like to thank the Graduate School of the University of Minnesota for financial research assistance, access to geologic literature, and the opportunity to continue my education.

INTRODUCTION

Purpose of Study

This study is an investigation of a sequence of Upper Cretaceous sedimentary rocks that have been interpreted as a deltaic complex. Two primary objectives were to determine paleocurrent patterns and to further delineate the provenance of the sequence. Detailed stratigraphic, petrologic, and petrographic information should invoke comparisons with similar depositional systems elsewhere.

Study Area

The field area lies in southwestern Wyoming near the town of Kemmerer, in the south-central portion of Lincoln County. Excellent natural exposures are plentiful, and artificial cuts are accessible in a large open pit coal mine owned by the P&M Mining Company. Specifically, this study looks at exposures between 41°37′ 50″ N to 41°38′30″ N and 110°37′30″ W to 110°37′ 15″ W. The total length, north to south, of the studied outcrop is 12 km and the width is 1 km. U.S. Highway 189 from Interstate 80 to Kemmerer generally parallels the natural exposures (Figure 1). Outcrops are accessible from roads leading west off U.S. Highway 189. Excellent outcrops of the Lazeart Sandstone Member are present at Crockers Point and Skull Point. The Adaville Formation is exposed in the coal pits.

Methods

Field work began on June 15, 1998 and ended on August 3,1998. Ten stratigraphic sections were measured using a 1.75 m Jacobs staff and a Brunton compass.

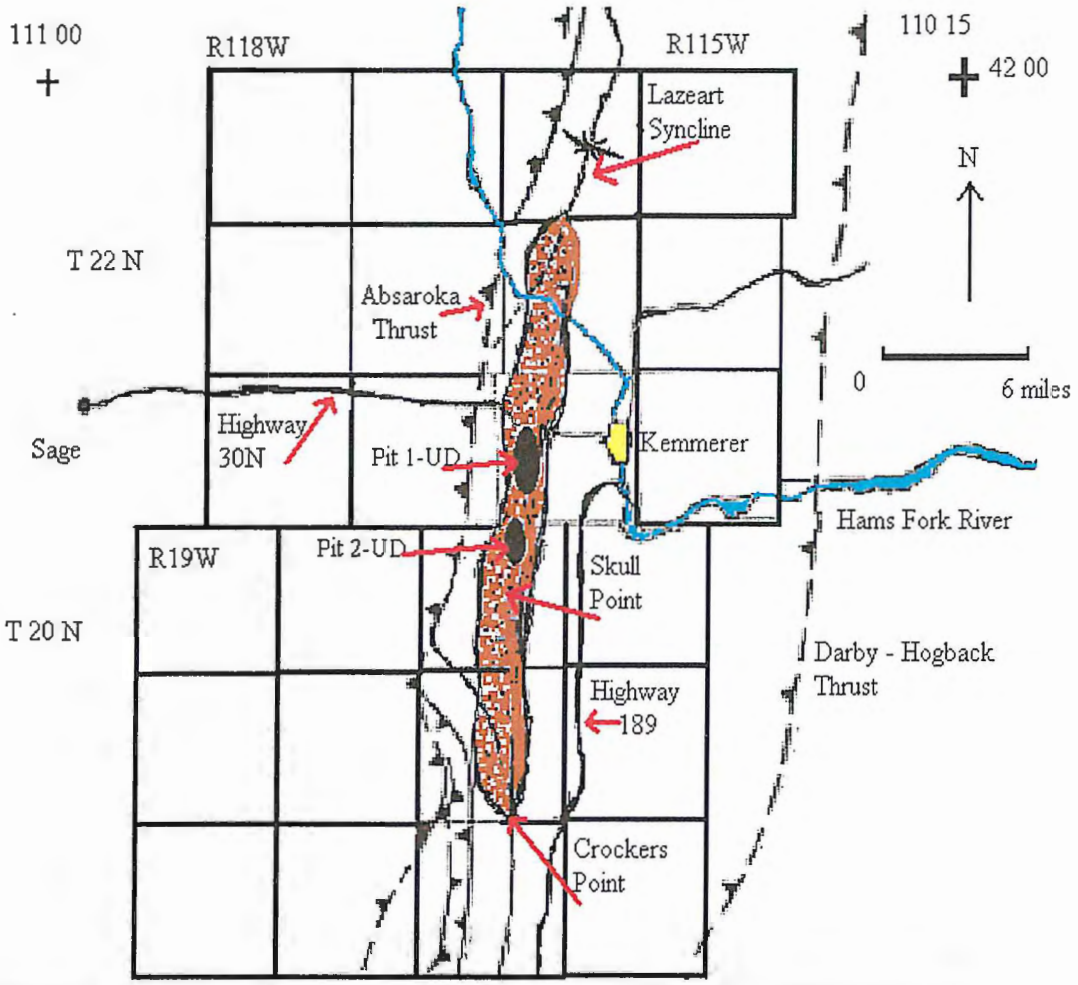

Figure 1. Location of study area in southwestern Wyoming. The brown area represents the studied portion of the Adaville Formation and its Lazeart Member. The black ovals represent two open pit coal mines owned by the P&M Mining Company. (After Lawrence, 1992, p. 71).

The sections were sampled at contacts, midsections, and depositional changes. Sample size ranged from 8 cm × 6 cm to 20 cm × 25 cm. Each sample taken was catalogued by its section and height within that section. Stratigraphic columns were constructed to show lithologic correlation between each section (Figure 2). Twenty continuous drill cores, 5 cm in diameter and ranging in length from 150 to 275 m, were sampled and analyzed.

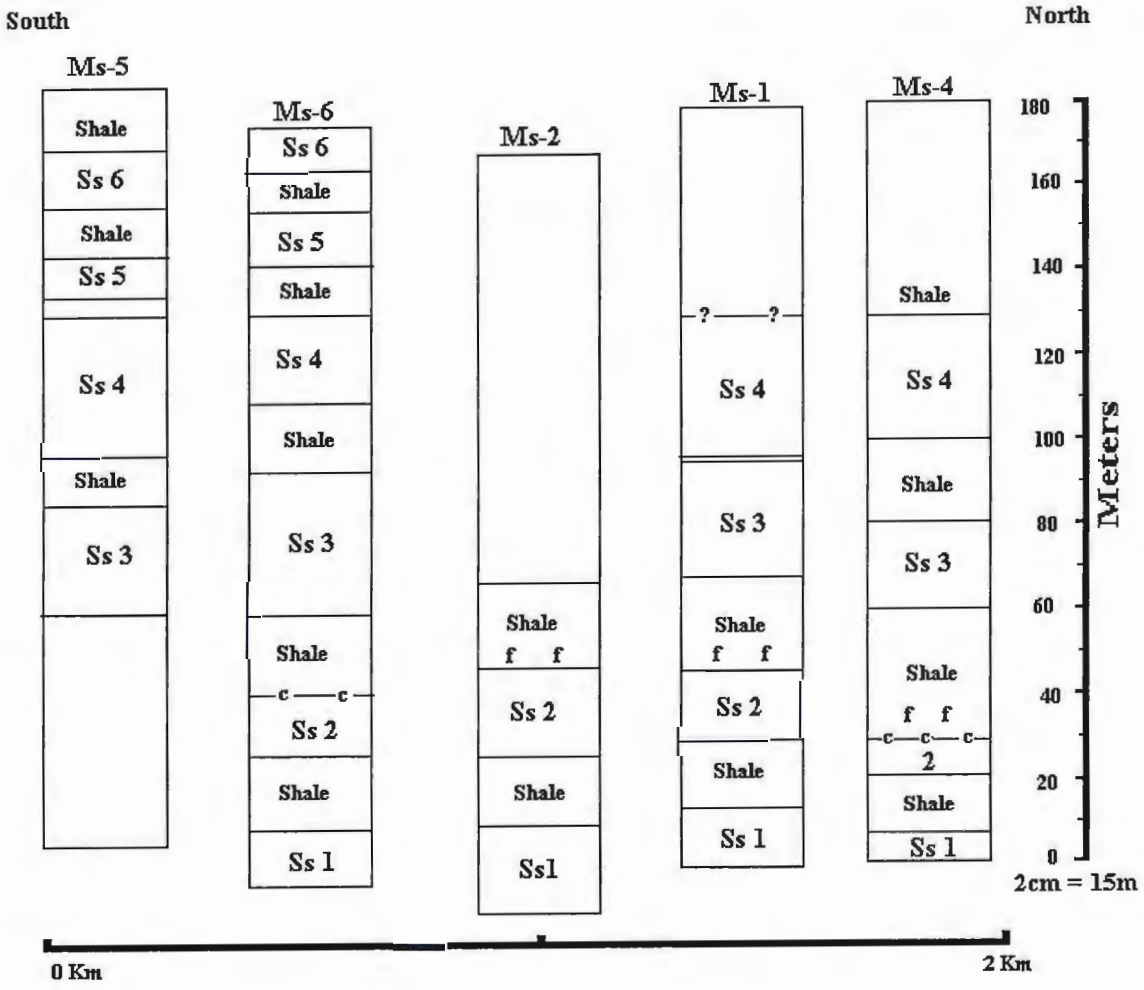

Figure 2. Geologic cross sections measured at Crockers Point. Sandstone bodies are separated by interbedded shale. The letter (f) indicates fossil horizons and the letter (c) indicates covered horizons.

The cores were obtained from a P&M Mining storage facility located in Frontier, Wyoming. The core data fully represent the coal-bearing strata of the lower Adaville Formation. Eight of the twenty studied cores extend into the Lazeart Member. Accompanying geophysical e-log data for the cores were available, but not utilized in this study.

Previous Work

The first Europeans to traverse the region were employees of the Rocky Mountain Fur Company - Gen. William Ashley, Capt. James Bridger, Capt. Robert Campbell, Capt. William Sublette, and Louis Vasquez. Captain Benjamin L.E. Bonneville was the first person to record and map regional geography from field excursions in 1834 and 1835 (Veatch, 1907). Although his work was to the north and west of this project's focus, he laid the groundwork for further exploration.

Capt. John C. Fremont in 1843 and Capt. H. Stansbury in 1849-50 further described the geologic and geographic attributes of this region. Fremont (1843) was the first to cite the presence of coal; he located coal beds near the Cumberland Gap and west of Oyster Ridge (Veatch, 1907). Fremont's discovery site lies approximately six miles south of the outcrops studied in this investigation. Stansbury (1852) added to the knowledge of coal in the region. He mapped coal beds on Sulphur Creek, Little Muddy Creek (Pivnik, 1990) at Cumberland and Reservoir Gap, and near the present city of Evanston. On his prepared maps, he labeled this region a "Great Coal Basin".

Henry Engelmann, a geologist from St. Louis, was the first to recognize Cretaceous strata in the region (1857). Englemann joined Capt. J.H. Simpson's company looking for new lines for the Pacific Railroad. On a traverse from Camp Floyd to Carson Valley, Englemann was able to complete a transcontinental profile from the Mississippi to the Pacific after linking data from previous expeditions together (Goetzmann, 1966). Englemann assigned a Cretaceous age to the Bear River, Benton, and Frontier Formations during a similar traverse between Fort Bridger, Wyoming and Coalville, Utah.

F. B. Meek, a paleontologist accompanying Capt. Simpson, disagreed with Englemann's Cretaceous classification. Meek believed the fossil record and presence of coal should classify the strata as a basal Tertiary unit (Veatch, 1907). This argument spawned the heated "Laramie problem". Many chronostratigraphic discussions took place regarding the coal-bearing strata of the Western Interior - were they Cretaceous or Tertiary? Veatch (1907, p.14) stated it best,

> "The region became one of the storm centers of the Laramie, Tertiary, Cretaceous discussion, since it contains the type locality of the Bear River Formation, here associated clearly with Cretaceous fossils, the leaf-bearing beds at Evanston on which Lesquereux based some conclusions, and, between the two, the type locality of the first vertebrate fossils found in the Wasatch."

Lesquereux (1878) believed the coal beds were of Tertiary age based on plant fossil information. The Bear River Formation continued to spur discussions until T.W. Stanton (1892) placed the formation as the lowermost Cretaceous unit in the region. The following year Stanton gave A.C. Peale's (1874) previously named Fox Hills Group a Colorado age, and renamed it the Frontier Formation (Veatch, 1907). Stanton's work, placing the Bear River Formation as the lowermost Cretaceous unit, took it out of the Laramie. By giving a Coloradian age to the Frontier, the overlying Hilliard Shale and Adaville Formation became part of the Cretaceous.

Stanton and F. H. Knowlton (1897) placed the Adaville Formation in the upper part of the Laramie. Using the work of L.F. Ward (1885) and current data, Stanton and Knowlton made the correlation on the basis of the great thickness of coal, lithologic character, general structure, and floral and faunal content (Lawrence, 1984). Stanton and Knowlton also regarded the shale underlying the Adaville to be marine due to its floral and faunal content. W. C. Knight (1902) also believed the coal-bearing beds of the

Adaville Formation should belong to the Laramie. He measured and described a section west of Kemmerer. From this section, Knight named the shale unit that separates the coal-bearing beds of the Frontier and Adaville Formations, the Hilliard Shale (Veatch, 1907).

Veatch (1907) did a formidable study of the Kemmerer area. He accurately described most of the stratigraphic units and structures. He also collected a representative fauna from the Adaville that was identified by Stanton. Veatch described the rocks of the Adaville as yellow, grey, and black carbonaceous clays with irregularly bedded brown and yellow sandstone. He named the basal white sandstone of the Adaville Formation the Lazeart Member. Veatch noted that the Evanston Formation unconformably overlies the Adaville with a conglomeratic unit, the Hams Fork Member. Finally, Veatch stated that the time gap between the Adaville and Evanston Formations represents a long period of folding, faulting, and erosion.

Veatch became interested in defining the age of the Evanston Formation. Dating the Evanston would help to determine the age of the Adaville and the timing of the Absaroka thrust event (Lawrence, 1984). Lesquereux previously listed the Evanston as Eocene, or possibly lower Miocene, based on floral content. Veatch thought the Adaville to be Eocene but felt more research was needed to verify this determination. Stanton, Knowlton, and Veatch continued to work on deciphering the age of the Adaville Formation by studying the fossil record. Using this information, Stanton regarded the Adaville as Montanian. Stanton also noted the depositional environment as brackish, based on lithology and fauna content. Knowlton's flora analysis determined the Adaville to be part of the Montana or Dakota Groups.

From 1937 to 1981, research on the Adaville Formation was concentrated on regional stratigraphy. Biostratigraphic studies were published by Cobban and Reeside (1962), Ruby et. al. (1961), Miller (1977), Nichols (1979), and Nichols and Jacobson (1981). Their studies indicated that the Adaville and its Lazeart Member are Late Santonian to Early Campanian, 84 to 80 m.y. old. Pryor (1961) petrographically analyzed the Mesaverde sandstones in Wyoming, including one sample of an Adaville sandstone. R.J. Weimer (1960) researched and described the regional rates of deltaic sedimentation within the Rocky Mountains. Lawrence (1984) extensively researched the Adaville Formation's total coal reserves, thickness, geometry, and distribution. Based on field research and geophysical data, Lawrence concluded that the Adaville Formation was deposited as a wave-dominated deltaic complex.

REGIONAL GEOLOGY

Introduction

Southwestern Wyoming's geologic history involves a complex series of events, including tectonism, sea level fluctuations, and sedimentation. The study area lies on the western edge of the Pomeroy Basin. This basin is tectonically bound by the Uinta Mountains to the south, Oyster Ridge to the east, the Wind River Range to the northeast, and a series of fold and thrust belts to the west. This project's focus is the Adaville Formation and its Lazeart Member. They are Upper Cretaceous sedimentary units deposited along the shoreline of an epicratonic sea (Figure 3).

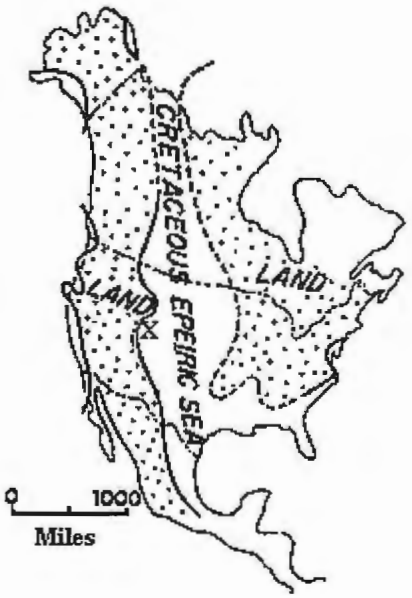

Figure 3. Map of the Cretaceous epeiric seaway in North America. The (X) marks the approximate location of the study area. (After Weimer, 1970).

Precambrian

The crystalline basement consists of igneous and metamorphic terrains within the Wyoming Archean province (Lush et. al., 1988). Precambrian outcrops are present in the Wind River, Gros Ventre, and Teton mountain ranges. Geophysical data do not show a direct relationship between the crystalline basement and the later thrusting events. The basement dips gently at four degrees to the west beneath a regional sole detachment within the Cambrian Gros Ventre Formation (Coogan and Royse, 1990).

Paleozoic

As Cambrian seas transgressed into the region, the first phase of sedimentation included the Flathead Sandstone, Gros Ventre Formation shale and limestone, and the Gallatin Limestone (Figure 4). Due to structural advances, the Flathead Sandstone is the only formation representing Cambrian sedimentation in western Wyoming. During Cambrian time the regional miogeocline received sediment from both the east and west (Armstrong and Oriel, 1965). Most of the Upper Cambrian through Devonian section is comprised of carbonates with minor interbedded shales and quartz arenites.

The Bighorn Dolomite represents an Upper Ordovician deposit in southwestern Wyoming. During the Ordovician, the study area was approximately on the land - water interface (Armstrong and Oriel, 1965). Consequently, sea to land interactions dominated depositional patterns throughout Paleozoic time. The stratigraphic sequence of southwest Wyoming does not contain any Lower to Middle Ordovician or Silurian deposits, but the fossil record of eastern Wyoming contains Ordovician and Silurian fauna and flora (Armstrong and Oriel, 1965). Thus, the absence of a complete Ordovician/Silurian

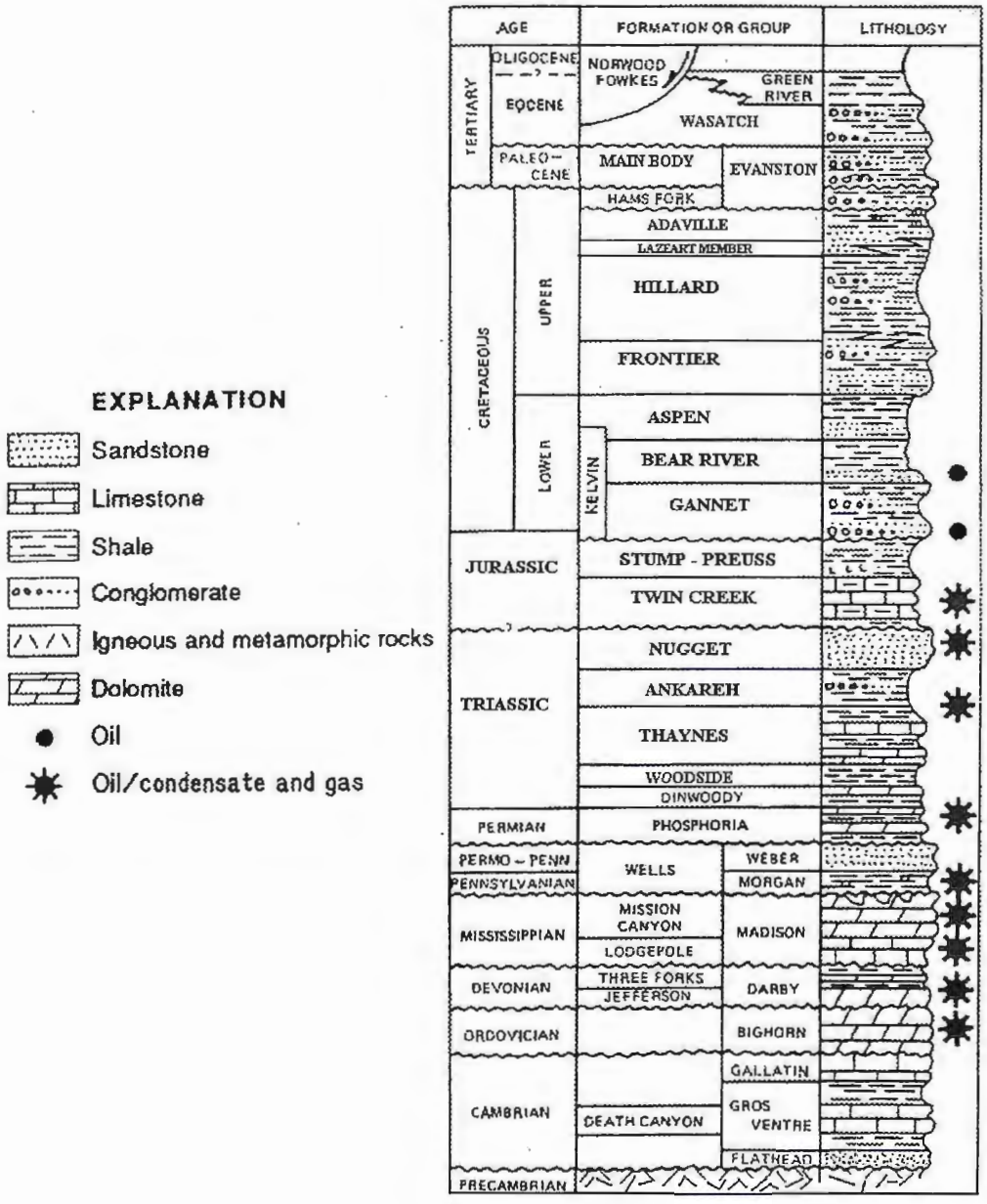

Figure 4. Stratigraphic column for the Wyoming-Idaho-Utah thrust belt. (After Lamerson, 1982).

record in the west is a consequence of periods of regional erosion rather than of non-deposition.

The second phase of sedimentation in southwest Wyoming began during the Mississippian and continued through Jurassic time. As depocenters progressively moved eastward, tectonic events such as the Mississippian Antler Orogeny (Speed and Sleep, 1982), the Pennsylvanian Ancestral Rocky Mountain uplift and the related Oquirrh basin subsidence (Jordan and Douglass, 1980) and the early Triassic Sonoma event (Carr and Paull, 1983) caused deposition to increase. The main type of sedimentation continued to be carbonate precipitation with interbedded layers of shale and sandstone. Both the Mississippian Madison Formation and the Rex Member of the Permian Phosphoria Formation contain chert-rich deposits.

Mesozoic

A third depositional stage placed tectogenic sediments into an elongated epicontinental Cretaceous foreland basin. During this stage of deposition, the western margin of the American plate was characterized by an Andean-type margin with the subduction of oceanic crust. Further inland, successive eastward- moving low angle thrusting events created the well-known Wyoming-Idaho-Utah thrust belt. The region contains nine major thrusts that young eastward: the Willard, Paris, Laketown, Meade, Crawford, Absaroka, Hogsback, Darby, and Prospect (Coogan and Royse, 1990). The Absaroka's movement thrust upward a section from the Ordovician Bighorn Formation through the Jurassic Twin Creek Formation (Figure 5). This tectonic event caused fresh clastic sediment to be shed into the rapidly subsiding adjacent foreland basin to the east.

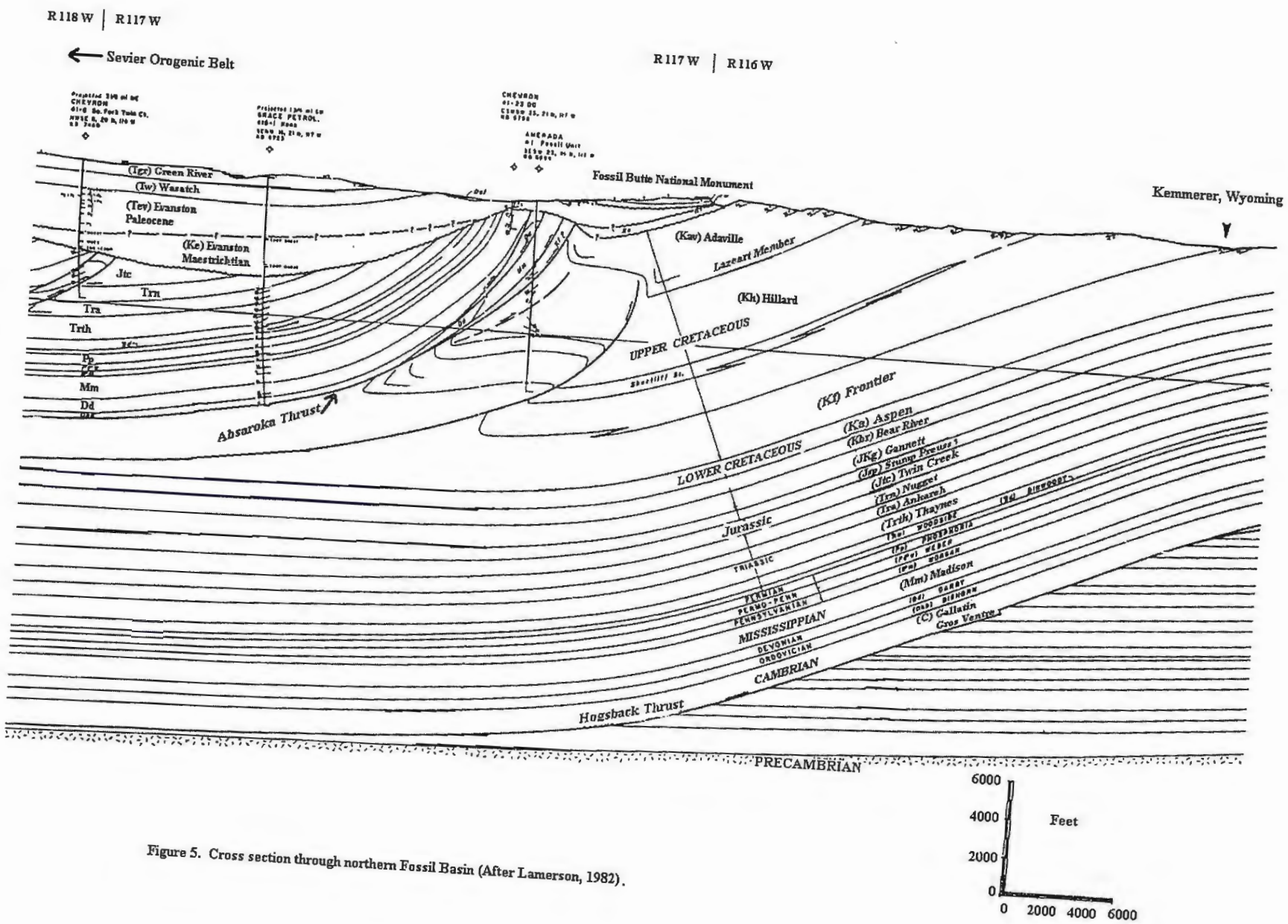

Figure 5. Cross section through northern Fossil Basin (After Lamerson, 1982).

. The Cordilleran highland and the exposed Absaroka Thrust sheets supplied the sediment for the Adaville Formation.

A period of Cretaceous transgressive-regressive pulses affected the depositional patterns of the western interior foreland basin (Rogers, 1998). The depositional basin of the Adaville Formation was subsiding at 200 m/m.y. while the maximum rate of sea-level fall was less than 50 m/m.y. (Kauffman, 1976, and Haq et al., 1987). During regressions, the Absaroka and older faults contributed sediment to a deltaic system prograding to the south-southeast. Thick organic-rich peat beds were deposited landward of the strandline. Peat bed accumulations were related to the magnitude of the regressive pulse. In general, global sea levels during the Late Cretaceous were on the rise (Figure 6).

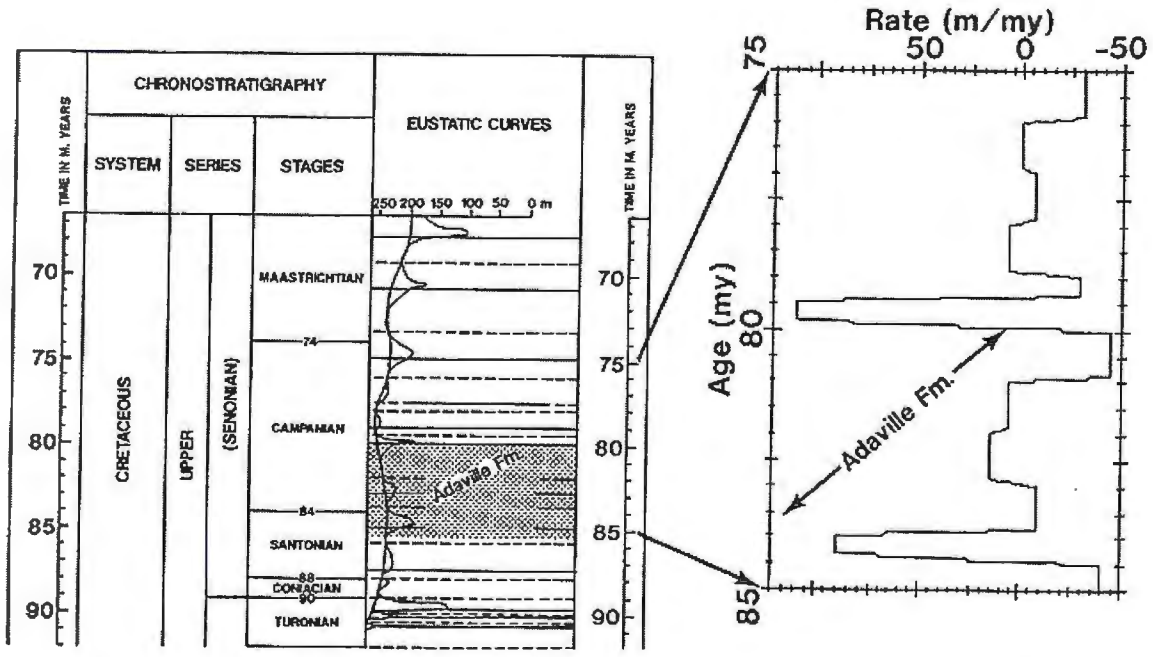

Figure 6. Part of a sea level curve prepared by Haq et. al. (1987) highlighting the deposition of the Adaville Formation during the late Santonian and Campanian. (From Lawrence, 1992).

Ryu and Neim (1999) have shown that the composition of petrographic framework grains may vary systematically from highstand and lowstand sea levels within depositional sequences. This suggests that relative sea level changes and tectonic uplift in the source area may affect patterns of sedimentation and sandstone composition.

Lawrence (1984) interpreted stacked sand bodies of the Lazeart Member, a minimal scouring depth of distributary channels, and the preservation of brackish water environments through 700 m to indicate a local base level rise during the deposition of the Adaville Formation. Tectonic activity was a major factor in the formation of the basin. Beaumont (1981) produced models showing a rapidly subsiding asymmetric trough forming adjacent to a series of frontal thrust sheets. The models show isostatic compensation in response to sediment load as a driving force behind foreland basin subsidence. Subsidence adjacent to the frontal thrust sheets is intensified by the weight of new sediment. Subsidence and sediment accumulation rates lessen basinward.

The end of the Cretaceous marks the final regression of the Cretaceous Sea in western Wyoming. This final regression was associated with the Laramide Orogeny. The Cretaceous basin underwent a period of uplift and subsequent erosion (Tweto, 1975). The Adaville Formation is unconformably overlain by the Hams Fork Conglomerate Member. The age of the Hams Fork Member is Cretaceous, but the main body of its parent formation, the Evanston, is Paleocene (Ruby et. al., 1975). Seventy years of fossil collections is the basis for the placement of this argumentative boundary.

Cenozoic

As the Late Cretaceous Sea regressed eastward, sediment continued to fill the western edge of the basin. Eventually, such processes moved the depositional high eastward, eliminating the miogeocline. During the Eocene, basin downwarping created a hydrogeographic low (Breithaupt, 1990). This newly formed basin gave rise to Lake Gosiute. Fed by many drainage systems from regional highlands, Lake Gosiute, a playa lake complex, grew to an estimated 40,155 square km (Surdam and Wolfbauer, 1975). Early Eocene sedimentologic and climatic variations led to changes in the lake's size and chemical composition. Variations of high and low lake levels are indicated in the Green River Formation. During Mid-Eocene time, Lake Gosiute was at a low stand and was eventually filled in with sediment from the Cordilleran Highland.

Oyster Ridge separated Lake Gosiute from two smaller western lakes within Fossil Basin during early Eocene time. This lake system contains one of the largest accumulations of lacustrine sediments in the world, the Green River Formation (Bradley, 1964). Fossil Butte National Monument, Fossil Lake's remnants, is a notable reserve for fish and plant fossils (Grande, 1984). Deposition of the Wasatch Formation simultaneously occurred with that of the Green River Formation. The Wasatch deposits often underlie or interfinger the Green River deposits. The fossil-rich Wasatch Formation contains a vast assortment of preserved mammals (Gazin, 1962).

Local Quaternary deposits consist of alluvium and gravel units. Local creeks – the Hams Fork, Little Muddy, Muddy, South Fork, and the Slate – transport alluvium. Alluvium deposits consist of unconsolidated massive to semi-stratified clay, silt, and sand

layers. Deposits predominately appear as channel fill and floodplain sediments. Pleistocene and Pliocene gravel deposits occur infrequently within the north-south trending Pomeroy Basin. The gravel consists of well-rounded quartzite, carbonate, and sandstone boulder- to cobble-sized clasts recycled from the Evanston Formation. The gravel deposits are locally as thick as 5 m.

Field Descriptions of Rock Units

Adaville Formation

The Adaville Formation is approximately 620 m thick and is considered to be Early Campanian in age (Lamerson, 1982). The lower half of the formation contains substantial economic coal seams. The seams are semi-continuous and range in thickness from 30 m to less than one meter. The coal predominately occurs as banded subbituminous deposits. Over a five-year period, the Adaville coal's average chemical and physical characteristics were: ash content 4.97 percent, sulfur content 0.67, moisture content of 21.31 percent, and an average BTU per pound of 9,847 (P&M Mining, 1997). Lawrence (1984) described the twenty most common lithologies within the Adaville Formation (Figure 7). The formation consists of 13 percent sandstone, 16 percent coal, and 71 percent mud to siltstone. Also within the Adaville are minor trough cross-beds, oyster deposits, normal faults, wave-induced ripples, bioturbated beds, and burned coal deposits (Figures 8 – 11).

Lazeart Member

This lower sandstone member of the Adaville Formation is approximately 180 m thick (M'Gonigle and Dover, 1992). The member forms large, approximately 25-m-high, north- south- trending cliffs at Crockers Point and Skull Point that dip westward at 22 to 25 degrees (Figures 12 and 13). Hand samples are fine- to medium-grained and moderately well-sorted. Nine measured stratigraphic sections of the Lazeart Member show six sand bodies separated by layers of silty shale. Fresh outcrops of the white

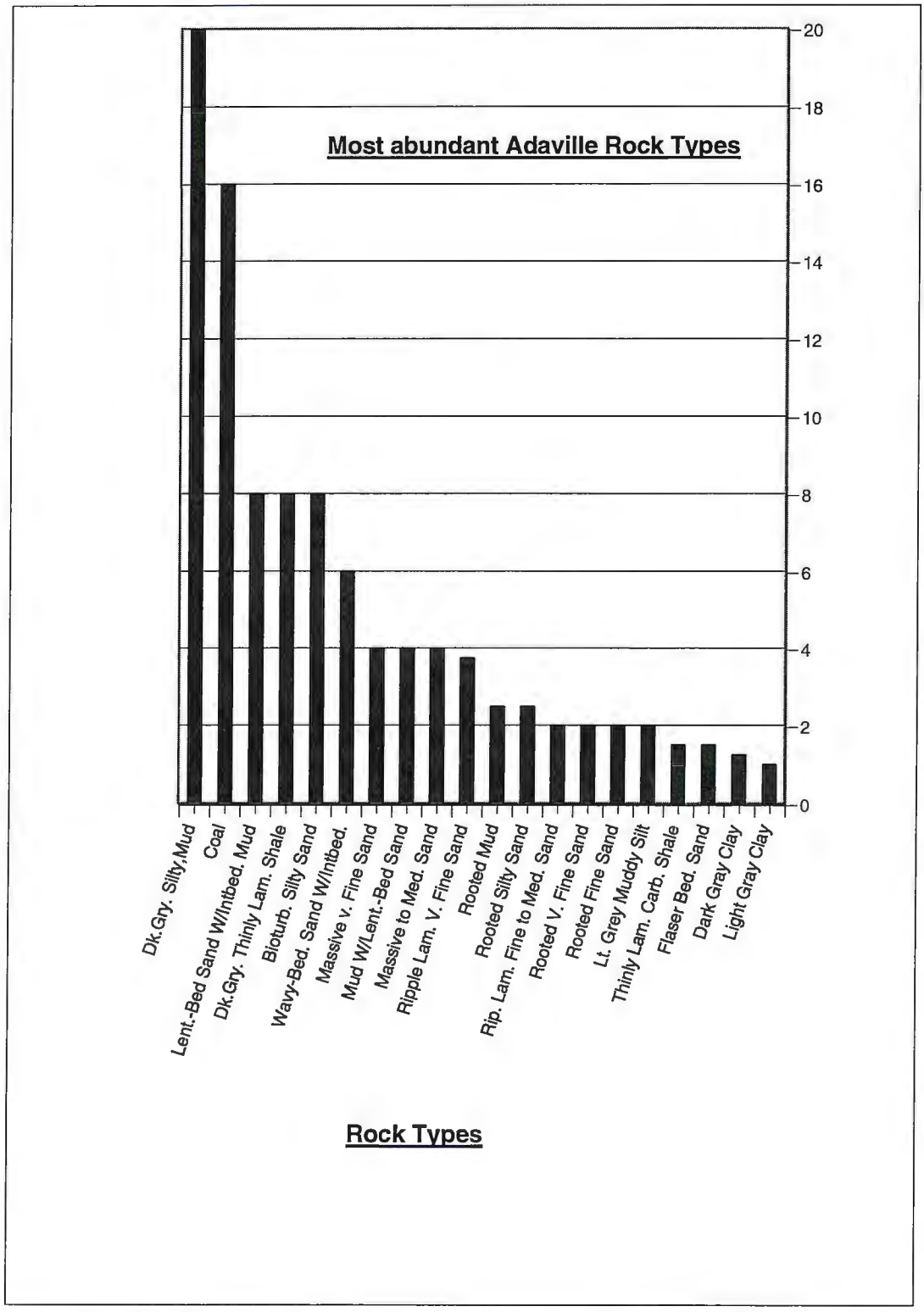

Figure 7. Rank abundance of the twenty most common rock types of the Adaville Formation. the percentage of coal (16 percent) in the section. (From Lawrence, 1982).

Figure 8. Photograph looking at the north wall of 1-UD pit. A prominent coal seam of the Adaville Formation splits into two just left of center. This coal seam is approximately 15 m thick. This view includes approximately 228 m of the total 385 m of the north wall. 1-UD is the largest coal pit operated by the P&M Mining Company near Kemmerer.

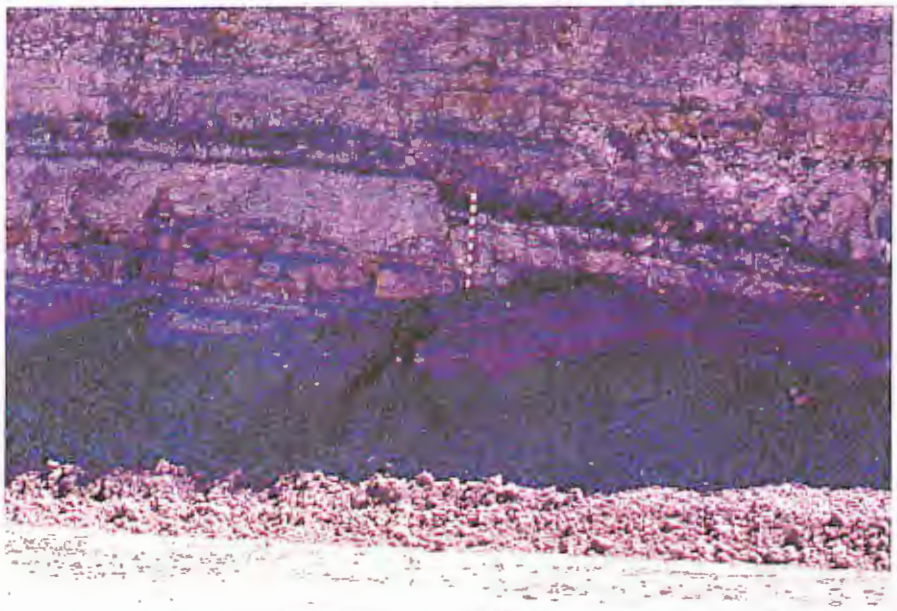

Figure 9. Photograph of a minor normal fault on the south wall of the 2-UD pit. The Jacob's staff is 1.75 m long. There are similar faults throughout this section of the Adaville Formation.

Figure 10. Photograph of oscillation ripple marks on top of a limonitic sandstone bed within the Adaville Formation at Crockers Point.

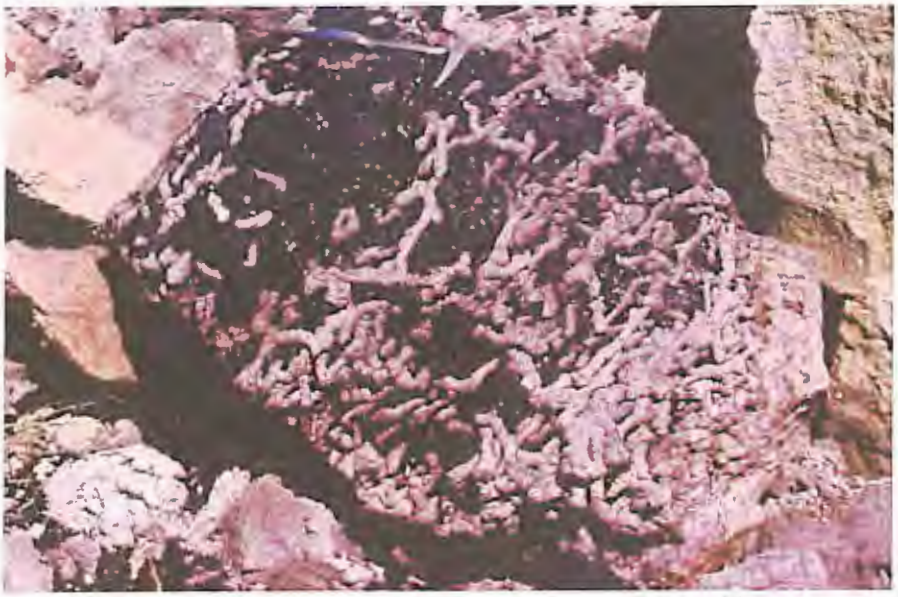

Figure 11. Photograph of extensive bioturbation within a thin coal seam of the Adaville Formation. This bioturbation occurs on the north wall of the 2-UD pit. A sandstone layer directly beneath the bioturbation is petroleum-saturated. Note rock hammer approximately 40 cm in length for scale.

Figure 12. Photograph approximately a half-mile north of Crockers Point, shows the cliff-forming Lazeart sandstones and the slope-forming interbedded shales. The field of view is approximately 240 m across.

Figure 13. Photograph of a Lazeart sandstone unit a quarter of a mile north of the Skull Point Mine. The sandstone cliff is 32 m in height.

sandstone characteristically have a "salt and pepper" appearance. Outcrops that exhibit iron-oxide staining have a yellowish-brown color. Iron-rich concretions appear in tear-drop forms and are as large as 1.6 m × 1.2 m. Calcite-cemented sub-spherical concretions as large as 0.3 m also occur, especially in the basal sandstone body. The basal and upper sand bodies are highly cross-bedded. Cross-bedding is commonly of the trough type, although there are rare occurrences of hummocky and herringbone types (Figures 14 and 15). Trough cross-bed sets range in height from 10 cm to 1.2 m. Rare hummocky cross-beds have sets of highly variant paleocurrent directions. Hummocky cross-bed sets averaged 22 cm in height and 4 m in length. Other features within the Lazeart sand bodies are flame structures, and wave-induced ripple marks. The reddish-brown silty shale layers between sand bodies commonly contain localized concentrations of gypsum and sulfur.

The shale layer directly above the second sand body contains a concentration of fossils including the bivalves Inoceramus, Exogyra, Crassostrea, Tellina, Flemingostrea, Crassostrea, Cymbophora, Plicatula, Protodonax, Sensis, and Pseudomleania. Ammonites include Baculites and Placenticeras. Trace fossils found include Skolithos, Thalassinoides, Ophiomorpha, and rare Teichicnus (Lawrence, 1992).

Figure 14. Photograph of trough cross-bedding from the basal sand body of the Lazeart Member at Crockers Point. Each change in color on the Jacob's Staff is a decimeter.

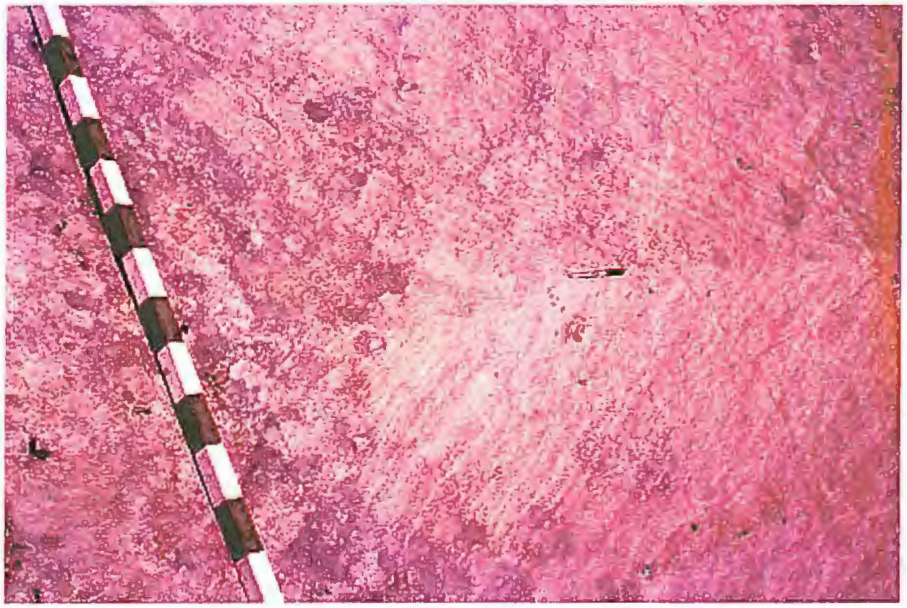

Figure 15. Photograph of herringbone cross-beds, 171° apart, from the basal sand body of the Lazeart Member at Crockers Point. The Jacob's Staff is divided into decimeters.

PETROGRAPHY

Thin Section Preparation

Forty-nine representative sandstone samples from the studied outcrops and cores were made into thin sections. Sampling goals were to represent each lithology, vertically and laterally, and to also sample beds that contain paleocurrent indicators in order to correlate composition and provenance. Of the forty-nine samples, twenty-three represent the Adaville Formation and the remaining twenty-six represent its lower Lazeart Member. The samples were cut perpendicular to bedding. Mineral oil had to be used as a cutting fluid due to high clay content within the samples. The sections were vacuum-impregnated and set with blue epoxy to make pore space more evident. Sodium cobaltinitrite was used to stain half of each section to make potassium-rich grains including K-feldspar and felsic volcanic rock fragments, stand out as yellow grains. Finally, each thin section was fitted with a permanent glass cover slip.

Classification and Descriptions

This project's classification scheme is based on a Qm:F:Lt triangular compositional diagram (Figure 16). On this triangle, (Qm) is equivalent to monocrystalline quartz grains, (F) represents both plagioclase- and potassium-feldspar grains, and (Lt) represents all fine-grained rock fragments including polycrystalline quartz and chert. The coarse-grained plutonic rock fragments (Plut. K-Q) were not added to the (Lt) pole. Instead, the amount was divided equally between the orthoclase and

Operational Definitions

Following is a list of grain characteristics.

Quartz

Common

Single crystalline grains exhibiting a sharp and complete extinction with less than one degree of rotation.

Undulose

Single crystalline grains exhibiting complete extinction between one and five degrees of rotation. Such grains commonly contain needle-shaped inclusions and or various amounts of vacuoles.

Polycrystalline

Grains containing numerous individual sub-crystals that undergo extinction at varying degrees of rotation. Some grains exhibit elongated sub-crystals. Subcrystals may have straight or undulose boundaries with adjacent grains.

Volcanic

Single crystals with sharp extinction and embayments that contain fine-grained volcanic matrix.

Feldspar

Orthoclase

Subhedral grains with low relief and a cloudy appearance. Stained grains are yellow. Altered orthoclase grains show

increased relief and vacuolization, dissolution along planes of cleavage, and replacement by clay minerals.

Plagioclase

Subhedral crystals showing albite twinning. Some are fresh and others are altered.

Microcline

Subrounded equidimensional crystals showing cross-hatched twinning patterns (albite and pericline twinning).

Rock Fragments

Volcanic, felsic

Subrounded grains containing a very fine-grained dark felsic crystalline matrix. Stained yellow by sodium cobaltinitrite.

Plutonic (K-Q)

Subrounded grains that contain sub-angular quartz grains and smaller amounts of orthoclase.

Metamorphic schist

Subrounded grains exhibiting elongation and common parallelism of quartz and mica crystals. Such fragments are relatively competent and are not affected by compaction.

Metamorphic, argillite and slate

Fine-grained groundmass with aligned grains and small mica grains.

Metamorphic, rock fragments

Subrounded grains containing non-aligned micas, and quartz grains (i.e. non-schistose).

Sedimentary mud-siltstone

Reddish brown to tan fragments containing small quartz inclusions, mica, and various clay minerals. Fragments are commonly deformed by compaction.

Sedimentary sandstone

Sandstone containing subangular to surrounded quartz grains set within a fine-grained matrix.

Carbonate fragment

Colorless to brownish subangular grains with well-defined rhombohedrons.

Chert

There are numerous combinations of polycrystalline mega- and microquartz detrital chert fragments. Some grains are chalcedonic. A few chert grains contain dolomite rhombohedroens.

Miscellaneous Grains

Biotite

Brown, somewhat pleochroic, and commonly deformed by compaction.

Muscovite

Colorless, moderately birefringent, and commonly deformed by compaction.

Opaques

Pyrite, hematite, and magnetite; commonly occurs in clusters.

Organics

Dark red, brown, to black fragments occur in coaly seams.

Matrix\Cement\Pore Space

Quartz cement

Authigenic silica overgrowths on existing quartz grains. In optical continuity with detrital grains. Quartz overgrowths predominately occur at grain contacts.

Chert cement

Very fine polycrystalline pore fillings. It is difficult to differentiate from very fine kaolinite cement, but the chert has a refractive index that is less than quartz and kaolinite's refractive index is greater than quartz.

Carbonate cement

Dolomite cement exhibits a moderate to high relief, weak rhombic infrastructure, a lack of twinning. Calcite cement

is colorless, birefringent, and commonly has lamellar twins.

Clay cement

Authigenic clay films coating detrital grains exhibit moderate birefringence.

Clay matrix

Ortho-, epi-, and pseudomatrix types are present in varying degrees; mixtures of kaolinite, illite, and sericite are typical.

Vermicular kaolinite cement

Authigenic well-developed "book" structures filling preexisting pore space. Low birefringence. Non-vermicular kaolinite is part of the clay matrix.

Pore space

Filled with bright blue epoxy.

quartz; the amounts were very small. Thirty-five thin sections were point counted, with six hundred points per slide.

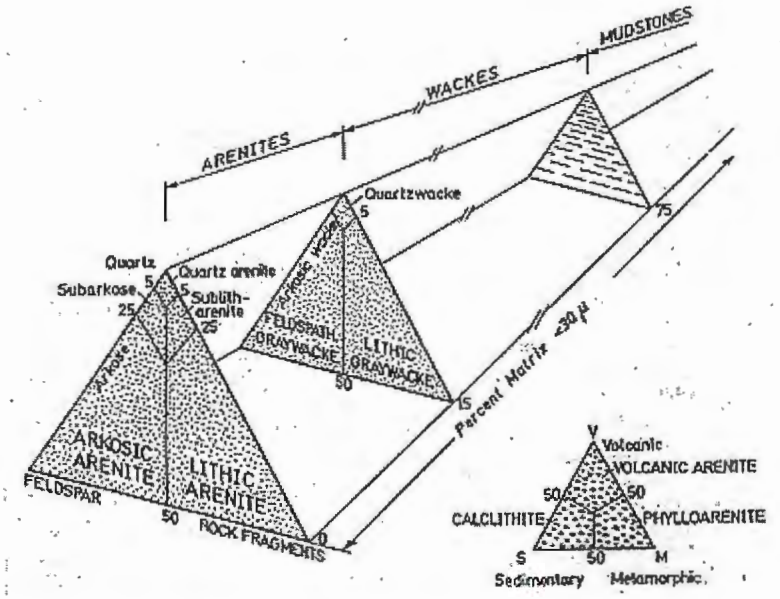

Figure 16. Classification of sandstones, a ternary QmFLt diagram. (From Pettijohn et. al., 1987).

Adaville Formation

Sandstones within the Adaville proper are very fine to fine-grained sub-mature deposits. Based on five thin sections, the Adaville's average Qm:F:Lt index is 71: 10: 19 (Table 1). Using the previous index, the Adaville sands are feldspathic sublitharenites and feldspathic litharenites (Figure 17). The average porosity is 6.3 percent. Monocrystalline quartz grains are subangular to sub-rounded and dominantly undulose. Unaltered orthoclase is the most common form of feldspar with minor amounts of altered orthoclase and mircocline. Rock fragments constitute 19.8 percent of the whole Adaville analysis. The most common rock fragment is chert, with minor amounts of felsic

		c8869,11m	c8869,41m	c8869, 71m	Ms-8,1m	Ms-8,13m
Quartz:	Common	1.0	1.8	1.5	3.0	5.7
	Undulose	41.7	36.2	36.8	39.3	36.7
	Polycrystalline	0.0	1.7	1.7	2.2	0.7
	Volcanic	0.0	0.0	0.0	0.0	0.0
	Total quartz	42.7	39.7	40.0	44.5	43.0
Feldspar:	Orthoclase	7.8	3.7	6.0	3.7	4.2
	Alt. ortho.	0.8	0.7	0.3	1.5	0.0
	Plagioclase	0.0	0.0	0.0	0.0	0.2
	Alt. plag.	0.0	0.0	0.0	0.0	0.0
	Microcline	0.0	0.0	0.2	0.0	0.3
	Total feldspar	8.7	4.3	6.5	5.2	4.7
Rock Frags:	Vol. Felsic	0.0	0.8	0.0	0.7	0.0
	Plut. K-Q	0.0	0.0	0.0	0.7	0.2
	Met. schist	0.0	0.3	0.0	0.5	0.0
	Met. arg.-sl	0.0	0.0	0.0	0.0	0.0
	Meta-frag	0.0	0.2	0.0	2.3	1.3
	Sed. mud-silst	0.0	0.2	0.0	0.3	0.0
	Sed. ss	0.0	0.2	0.0	0.2	0.0
	Carb. frag.	2.3	0.0	0.0	0.0	0.0
	Chert	5.8	5.2	4.5	11.7	14.0
	Total RF	8.2	6.8	4.5	16.3	15.5
Misc. grains:	Biotite	0.3	0.0	0.0	0.0	0.0
	Muscovite	0.5	0.5	0.0	0.0	0.0
	Opaques	0.5	0.0	0.0	0.3	0.8
	Organics	3.0	5.5	0.0	0.0	0.5
Matrix/Cement:	Cement,quartz	2.0	1.8	2.0	3.2	0.0
	Cement, chert	0.0	0.0	0.0	1.8	0.7
	Cement, carb	0.0	0.0	47.0	0.0	34.8
	Cement, clay	2.5	3.8	0.0	1.0	0.0
	Matrix, clay	25.5	28.2	0.0	9.5	0.0
	Vermic. kaolin.	0.2	1.0	0.0	1.0	0.0
	Total cem/mat	30.2	34.8	49.0	16.5	35.5
	Pore space	6.0	8.3	0.0	17.2	0.0
	Total	100.0	100.0	100.0	100.0	100.0
	Qm:F:Lt	75:09:16	75:13:12	64:08:28	70:10:20	67:07:26

Table 1. Modal analyses of sandstones within the Adaville Formation. (Ms) represents a measured section and (c) represents a core. The number identifies the particular measurement and the meters represent the height or depth within that section.

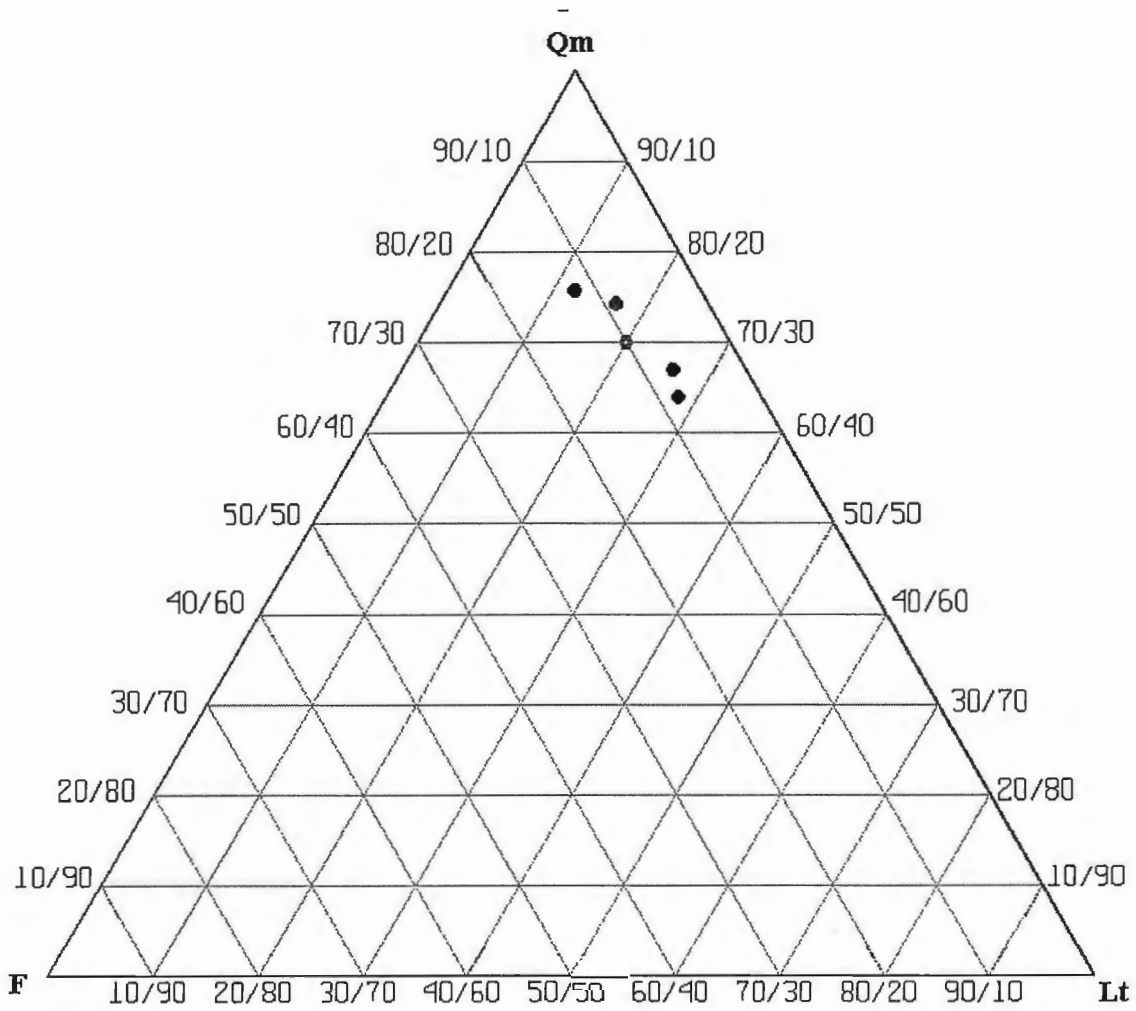

Figure 17. Ternary QmFLt diagram of 5 modal analyses of sandstones from the Adaville Formation.

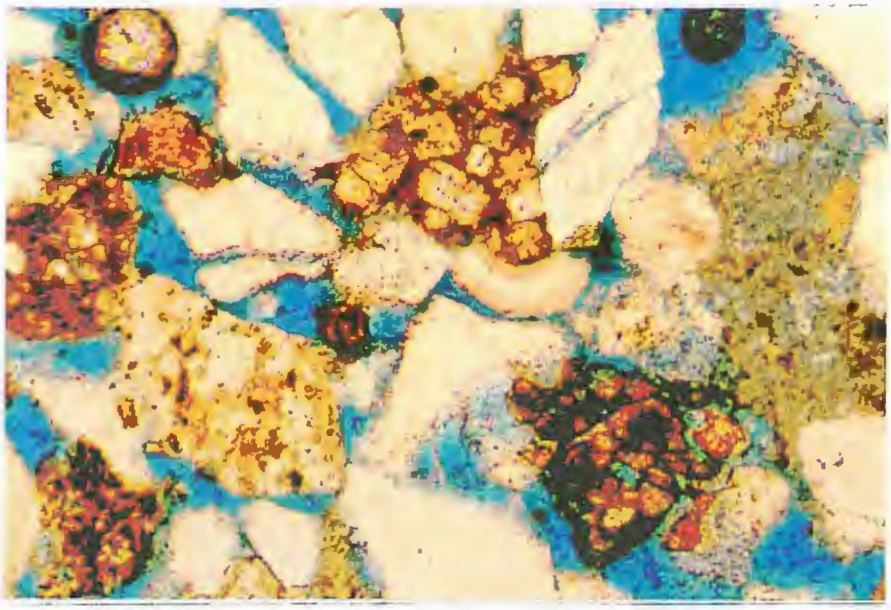

Figure 18. Photomicrograph showing dolomite rhombs (upper center), K-feldspar (yellow), an agate (center), quartz, clay matrix, and pore space (blue). Adaville Formation, core 8410, 83 m. Plain light. Field of view is 1.0 mm wide.

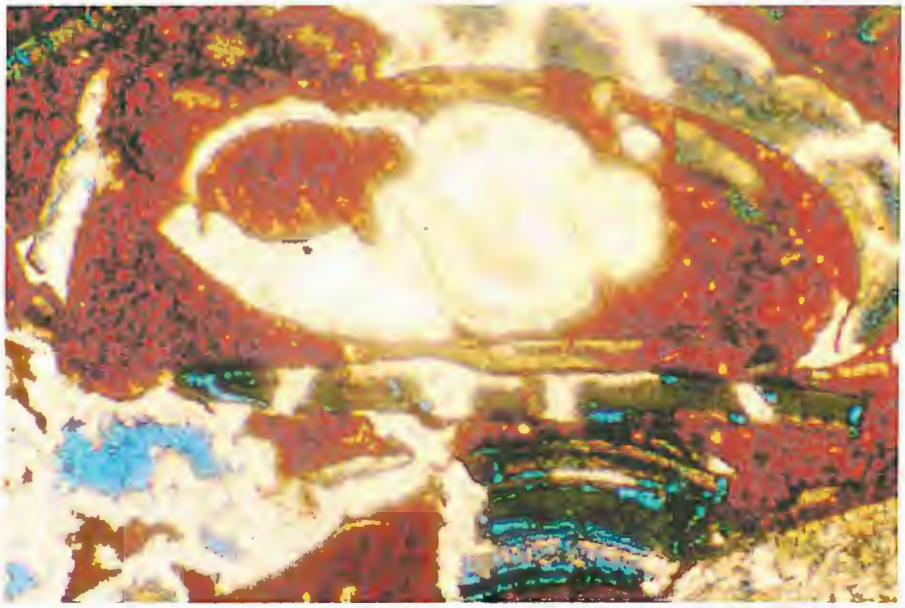

Figure 19. Photomicrograph of an oyster bed within the Adaville Formation. Shell fragments set in a matrix of brown silty mudstone. Plain light. Field of view is 2.5 mm wide.

volcanic and metamorphic fragments, and polycrystalline quartz. Organics occur in the form of thin laminae and fragments. The sandstones are generally held together by either carbonate cement or a clay matrix (Figure 18). Oyster beds within the Adaville are comprised of fossil fragments embedded in a reddish brown silty mudstone (Figure 19). Minor amounts of quartz cement, chert cement, and vermicular kaolinite locally affect sandstone competency.

Lazeart Member

The Lazeart sandstones are fine-grained and sub-mature. Average Qm:F:Lt index is 58: 10: 32 based on thirty thin sections (Table 2). This index classifies the Lazeart sandstones as feldspathic lithic arenites, feldspathic sublitharenites, and feldspathic arenites (Figure 20). The average porosity is 12.6 percent. Undulose subangular to subrounded quartz grains make up 33 percent of the studied samples. Some of these undulose quartz grains contain needle-shaped inclusions of rutile, actinolite, and sillimanite. Orthoclase is the most common feldspar, totaling approximately 6 percent (Figures 21 and 22). Altered orthoclase, microcline, and plagioclase occur in minor amounts (Figures 23 and 24). The lithic index of 32 is mainly comprised of dark chert grains (Figures 22 and 25). The abundance of such particles gives the sandstones of the Lazeart Member a "salt and pepper" appearance. Other lithic components are polycrystalline quartz grains, mud-siltstones, and schistose to non-schistose metamorphic fragments. The competence of sandstones within the Lazeart Member is dependent on the amount of clay matrix or carbonate cement (Figure 26). Samples from sand body number two have the most carbonate cement. The remaining

		Ms-1, 6.5m	Ms-1, 31m	Ms-1,43m	Ms-1, 96m	Ms-2, 18m	Ms-3, 5m	Ms-3, 24m	Ms-3, 45m	Ms-3, 57m	Ms-4, 79m	Ms-4, 97m	Ms-4,112m	Ms-4, 170m	Ms-6, 1m
Quartz:															
	Common	2.7	16.5	8.5	2.2	2.2	2.0	1.0	0.8	0.0	0.7	4.3	2.5	2.7	1.5
	Undulose	32.2	31.8	31.3	33.0	33.0	31.2	38.0	30.0	31.2	38.0	33.5	35.8	26.2	34.8
	Polycrystalline	1.5	2.7	0.8	3.0	3.0	1.2	2.0	0.8	2.0	0.5	0.3	1.0	0.0	1.7
	Volcanic	0.0	0.2	0.0	0.0	0.0	0.0	0.0	0.0	0.0	0.0	0.0	0.0	0.0	0.0
	Total quartz	48.7	61.5	57.8	49.5	49.5	43.3	45.8	42.3	45.8	50.7	47.7	51.3	30.2	53.5
Feldspar:															
	Orthoclase	5.3	4.0	6.2	6.5	6.5	8.7	8.3	10.3	8.3	6.2	3.3	3.0	13.5	5.8
	Alt. ortho.	1.8	1.3	0.7	1.5	1.5	1.3	0.7	0.3	0.0	0.0	1.2	1.0	1.7	0.8
	Plagioclase	0.0	0.0	0.0	0.0	0.0	0.0	0.0	0.2	0.0	0.2	0.0	0.0	0.0	0.2
	Alt. plag.	0.2	0.0	0.0	0.0	0.0	0.0	0.0	0.0	0.0	0.0	0.0	0.0	0.0	0.0
	Microcline	0.0	0.7	0.2	0.3	0.3	0.7	0.3	0.2	0.0	0.2	0.2	0.3	0.0	0.0
	Total feldspar	7.3	6.0	7.0	8.3	8.3	10.7	9.3	11.0	8.3	6.5	4.7	4.3	15.2	6.8
Rock Frags:															
	Vol. felsic	0.0	0.0	0.0	0.0	0.0	0.3	0.3	0.7	2.3	1.5	3.3	0.0	0.0	0.2
	Plut. K-Q	0.3	0.3	0.8	0.0	0.0	0.0	0.8	0.3	1.2	1.0	0.5	0.3	0.0	1.0
	Met. schist	0.0	0.3	0.0	0.7	0.7	0.8	0.0	1.0	1.0	2.0	2.2	1.3	0.0	0.7
	Met. arg.-sl	0.0	0.0	0.0	0.0	0.0	0.0	0.0	0.0	0.0	0.0	0.3	0.0	0.0	0.0
	Meta-frag	0.2	0.0	0.0	0.0	0.0	0.0	0.0	0.2	0.0	0.0	0.0	5.2	0.0	2.5
	Sed. mud-silst	3.3	1.5	2.2	2.3	2.3	4.3	2.0	5.5	8.7	3.7	2.2	5.3	0.2	3.0
	Sed. ss	0.0	0.2	0.2	0.0	0.0	0.0	0.0	0.0	0.0	0.0	0.0	0.0	0.0	0.0
	Carb. frag.	0.0	0.0	0.0	0.2	0.2	0.0	0.0	0.0	0.2	0.0	0.0	0.0	0.0	0.0
	Chert	12.3	10.6	17.2	11.3	11.3	9.0	4.8	10.7	12.7	11.5	9.5	12.0	1.3	15.5
	Total RF	3.8	3.0	3.2	3.0	3.0	5.7	3.2	7.7	13.2	8.3	8.5	12.2	0.2	7.3
Misc. grains:															
Misc. grains:	Biotite	0.2	0.2	0.0	0.2	0.2	0.5	0.0	0.2	2.0	1.0	0.0	0.0	0.0	0.2
	Muscovite	0.0	0.2	0.0	0.0	0.0	0.3	0.0	0.0	0.3	0.0	0.0	0.0	0.0	0.3
	Opaques	0.8	0.2	0.7	1.0	1.0	0.5	0.3	0.2	0.7	0.0	0.5	1.2	0.0	0.2
	Organics	0.0	0.2	0.0	0.0	0.0	0.2	0.0	0.0	0.0	0.0	0.0	0.0	0.0	0.0
Matrix/Cement:															
	Cement,quartz	2.7	0.0	0.0	4.0	4.0	4.5	4.7	1.7	2.2	4.0	5.0	4.2	0.0	3.3
	Cement, chert	4.0	1.8	0.0	0.7	0.7	0.2	0.5	0.3	0.2	0.0	0.0	0.0	0.0	0.0
	Cement, carb	0.0	24.8	28.5	0.0	0.0	0.0	0.0	20.0	1.5	0.3	0.0	0.0	54.0	0.0
	Cement, clay	1.2	0.0	0.0	0.0	0.0	0.0	1.2	0.0	0.0	0.0	0.0	0.0	0.0	0.0
	Matrix, clay	12.2	0.0	0.2	15.7	15.7	19.7	18.2	7.7	11.8	11.0	9.5	10.8	0.0	16.2
	Vermic. kaolin.	4.8	1.0	0.0	0.3	0.3	1.7	1.3	0.8	0.8	0.0	0.3	0.7	0.0	0.3
	Total cem/mat	24.8	27.0	28.7	20.7	20.7	26.0	25.8	29.7	16.5	15.2	15.0	15.7	54.0	19.7
	Pore space	14.3	1.6	2.7	17.2	17.2	12.8	15.5	8.2	13.0	18.3	23.8	15.3	0.5	11.8
	Total	100.0	100.0	100.0	100.0	100.0	100.0	100.0	100.0	100.0	100.0	100.0	100.0	100.0	100.0
	Qm:F:Lt	58:12:30	69:09:22	59:10:31	58:14:28	62:12:26	56:18:26	67:16:17	51:18:31	46:12:42	59:10:31	62:08:30	57:06:37	63:33:04	54:10:36

Table 2. Modal analyses of sandstones from the Lazeart Member. (Ms) represents a measured section and (c) represents a core.

		Ms-6, 9m	Ms-6, 64m	Ms-6, 91m	Ms-6, 155m	Ms-7, 1m	Ms-7,48m	Ms-7,76m	Ms-9,29m	Ms-9,32m	Ms-9,69m	Ms-10,80m	Con1,ln	Con1,out	Con1,rep	Lzss,sp1	Lzss,sp2
Quartz:	Common	0.7	0.0	4.3	2.5	2.7	3.7	2.7	3.7	2.7	1.0	2.3	10.2	2.2	1.7	0.2	1.2
	Undulose	38.2	30.8	44.8	35.2	25.2	36.0	39.0	25.5	26.7	32.7	30.7	25.8	32.8	27.2	38.2	40.2
	Polycrystalline	0.8	0.3	1.0	0.5	0.8	2.7	2.0	0.7	1.8	3.8	3.5	1.3	2.2	3.2	1.5	2.2
	Volcanic	0.0	0.0	0.0	0.0	3.7	0.0	0.0	0.0	0.0	0.0	0.0	0.0	0.0	0.0	0.0	0.0
	Total quartz	46.3	45.3	56.8	49.0	48.3	56.0	53.3	46.3	41.7	56.2	56.2	54.5	55.2	54.0	55.5	58.0
Feldspar:																	
	Orthoclase	5.5	6.2	2.8	3.5	5.3	1.2	3.7	8.5	6.8	4.7	6.0	3.3	3.5	2.8	3.3	1.8
	Alt. Ortho.	1.0	0.5	0.3	1.0	0.0	0.8	0.5	1.0	0.3	0.2	1.2	0.0	1.0	1.3	1.2	1.3
	Plagioclase	0.0	0.0	0.2	0.0	0.3	0.2	0.0	0.0	0.2	0.0	0.0	0.2	0.0	0.0	0.2	0.3
	Alt. Plag.	0.0	0.0	0.0	0.0	0.0	0.0	0.3	0.0	0.0	0.0	0.0	0.0	0.0	0.0	0.0	0.2
	Microcline	0.0	0.0	0.0	0.0	0.0	0.0	0.0	0.0	0.0	0.0	0.0	0.0	0.0	0.0	0.0	0.0
	Total feldspar	6.5	6.7	3.3	4.5	5.7	2.2	4.5	9.5	7.3	4.8	7.2	3.5	4.5	4.2	4.7	3.7
Rock Frags:																	
	Vol. Felsic	0.0	0.0	0.0	0.0	0.7	0.8	1.3	0.5	0.3	1.0	0.7	0.3	0.8	1.2	0.5	0.0
	Plut. K-Q	0.3	0.2	0.0	0.0	0.5	0.7	0.3	0.3	2.0	2.0	0.8	1.0	0.5	0.2	1.0	1.8
	Met. schist	0.5	1.2	0.3	0.2	0.5	0.8	1.0	1.0	1.8	1.7	0.8	0.7	1.0	1.2	2.2	1.3
	Met. arg.-sl	0.0	0.0	0.0	0.0	0.0	0.0	0.0	0.0	0.0	0.0	0.0	0.0	0.0	0.0	0.0	0.0
	Meta-frag	0.5	0.0	0.5	1.8	0.2	1.5	1.7	2.3	3.3	1.3	1.2	0.5	2.5	1.0	2.5	2.3
	Sed. mud-silst	2.3	3.3	0.3	1.8	1.8	0.8	0.3	1.3	0.8	0.3	2.0	0.2	0.7	0.5	1.5	2.0
	Sed. ss	0.3	0.2	0.0	0.2	3.0	1.8	0.3	0.0	0.2	0.2	0.5	0.0	0.0	1.0	0.5	0.7
	Carb. Frag.	0.0	0.0	0.0	0.0	0.0	0.0	0.0	0.0	0.0	1.8	0.0	0.0	0.0	0.0	0.0	0.0
	Chert	6.7	14.2	6.7	10.8	16.0	13.7	9.7	16.5	10.5	18.7	19.7	17.2	18.0	22.0	15.7	14.5
	Total RF	4.0	4.8	1.2	4.0	6.7	6.5	5.0	5.5	8.5	8.3	6.0	2.7	5.5	5.0	8.2	8.2
Misc. grains:			0.0														
	Biotite	0.0	0.5	0.2	0.0	0.7	0.0	0.0	0.5	2.0	0.0	0.0	0.0	0.0	0.2	0.0	0.2
	Muscovite	0.0	0.5	0.0	0.0	0.2	0.0	0.2	0.0	0.2	0.0	0.2	0.0	0.2	0.0	0.3	0.3
	Opaques	0.3	0.7	0.0	0.3	1.2	0.0	0.5	0.0	2.0	0.0	0.2	0.2	0.3	0.5	0.0	0.7
	Organics	0.0	0.0	0.0	0.0	0.0	0.0	0.0	0.0	0.0	0.0	0.0	0.0	0.0	0.0	0.0	0.0
Matrix/Cement:																	
	Cement,Quartz	3.5	1.8	3.2	1.2	1.8	2.2	3.2	0.0	0.8	0.7	1.8	0.0	0.3	1.3	1.2	1.5
	Cement, Chert	0.7	2.7	0.5	0.3	1.3	3.2	1.5	0.0	0.0	0.0	1.5	0.0	1.3	0.3	0.2	0.3
	Cement, carb	0.0	0.0	0.0	0.0	0.0	0.0	0.0	38.2	0.0	0.0	0.0	39.2	0.0	0.0	0.0	0.0
	Cement, Clay	0.0	0.0	0.0	0.0	0.0	0.5	0.0	0.0	0.0	0.0	0.0	0.0	0.0	0.0	0.0	0.0
	Matrix, clay	19.8	15.0	10.0	21.8	19.3	16.2	15.0	0.0	13.2	11.7	11.3	0.0	9.8	12.5	9.2	9.3
	Vermic. Kaolin.	2.5	1.3	1.8	0.3	1.2	0.3	0.0	0.0	3.7	2.0	0.5	0.0	5.7	3.0	4.3	2.5
	Total Cem/mat	26.5	19.5	15.5	23.7	22.5	22.0	19.7	38.2	17.7	14.3	15.2	39.2	17.2	17.2	14.8	13.7
	Pore space	16.3	20.7	23.0	18.5	13.7	13.0	16.8	0.0	20.7	16.3	15.2	0.0	17.2	19.0	16.5	15.3
	Total	100.0	100.0	100.0	100.0	100.0	100.0	100.0	100.0	100.0	100.0	100.0	100.0	100.0	100.0	100.0	100.0
	Qm:F:Lt	68:11:21	54:12:34	80:05:15	66:08:26	52:09:39	61:04:35	######	48:15:37	51:13:36	48:07:45	48:10:42	59:06:35	46:06:48	54:07:39		59:05:36

Table 2. Modal analyses of sandstones from the Lazeart Member. (Ms) represents a measured section and (c) represents a core.

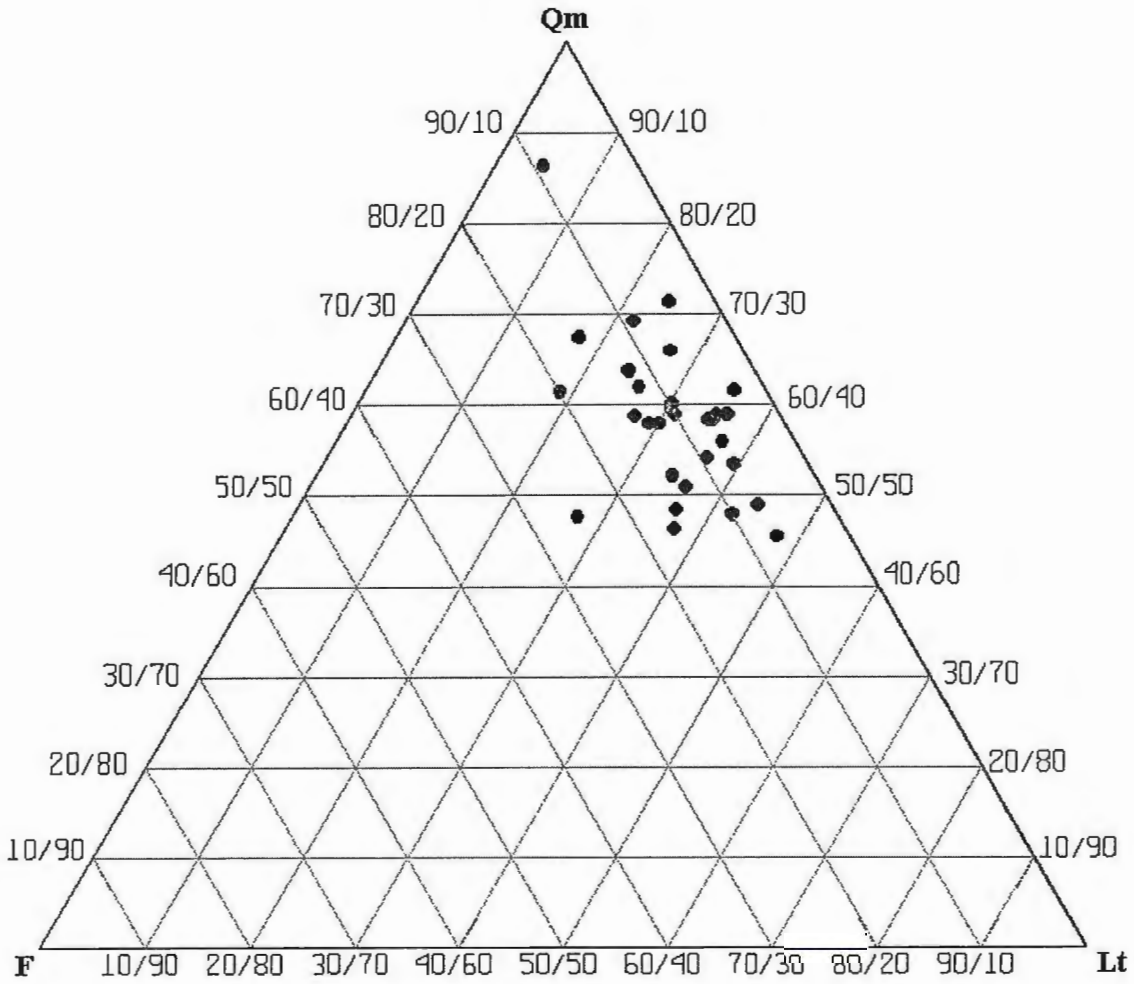

Figure 20. Ternary QmFLt diagram of 30 modal analyses of sandstones from the Lazeart Member.

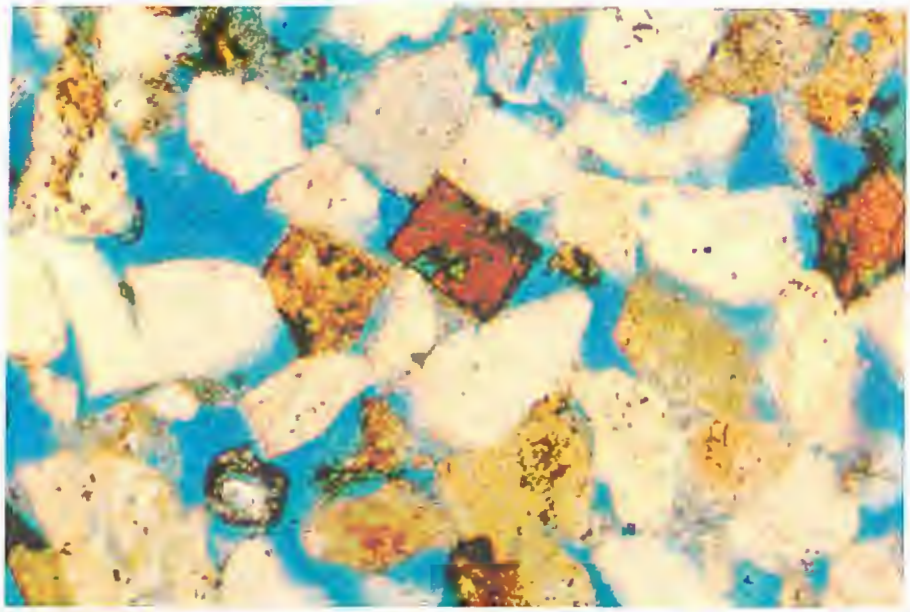

Figure 21. Photomicrograph of a rectangular K-feldspar grain (center) with subangular to subrounded quartz and chert. Lazeart Member, Sp-1, 110 m. Plain light. Field of view is 1.0 mm wide.

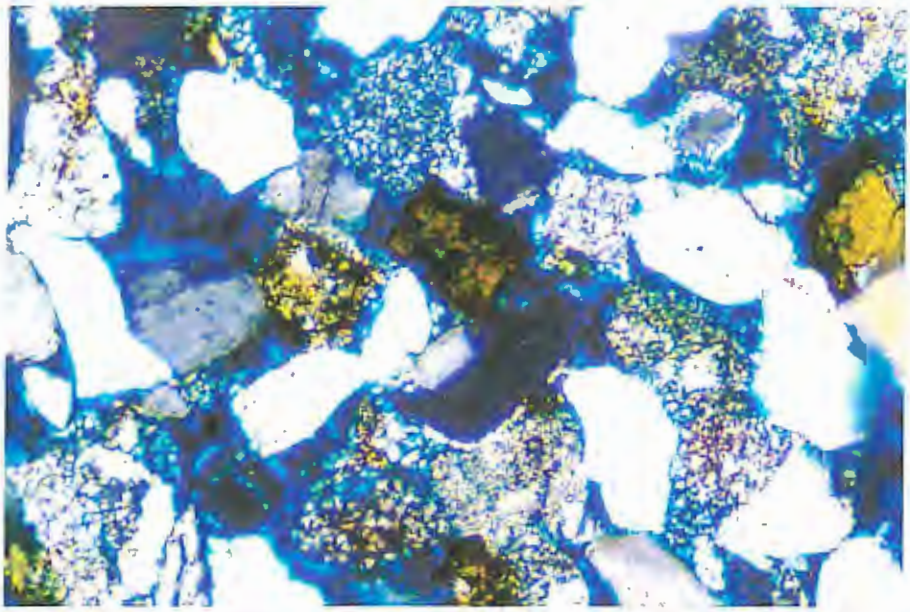

Figure 22. Photomicrograph of previous figure in crossed-polarized light. Note the abundance of chert grains (speckled). Field of view is 1.0 mm wide.

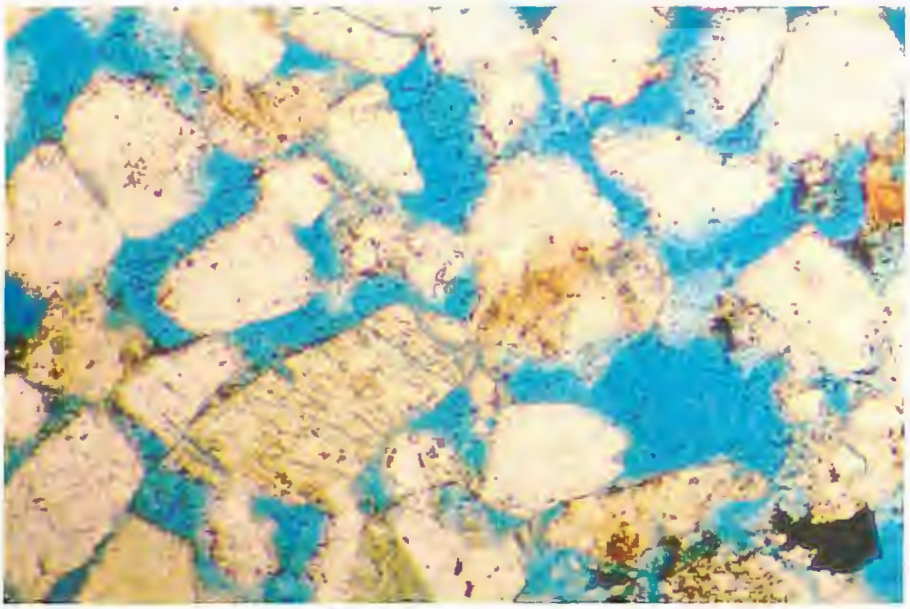

Figure 23. Photomicrograph of numerous chert and quartz grains. Adaville Formation, core 8292, at a depth of 89 m. Blue epoxy represents the pore space. Plain light. Field of view is 1.0 mm wide.

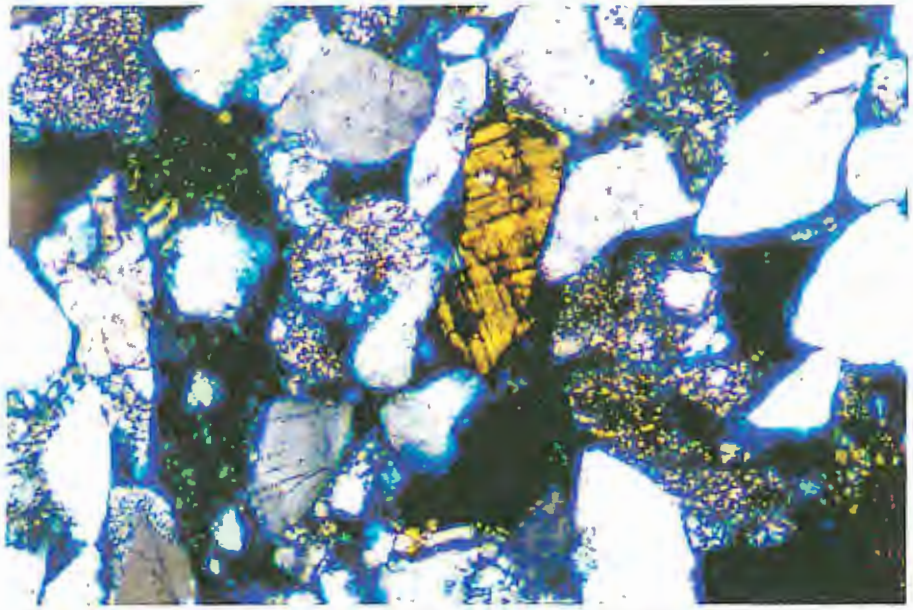

Figure 24. Photomicrograph of microcline, subangular quartz, and chert grains. Lazeart Member, Sp-2, 115m. Crossed-polarized light. Field of view is 1.0 mm wide.

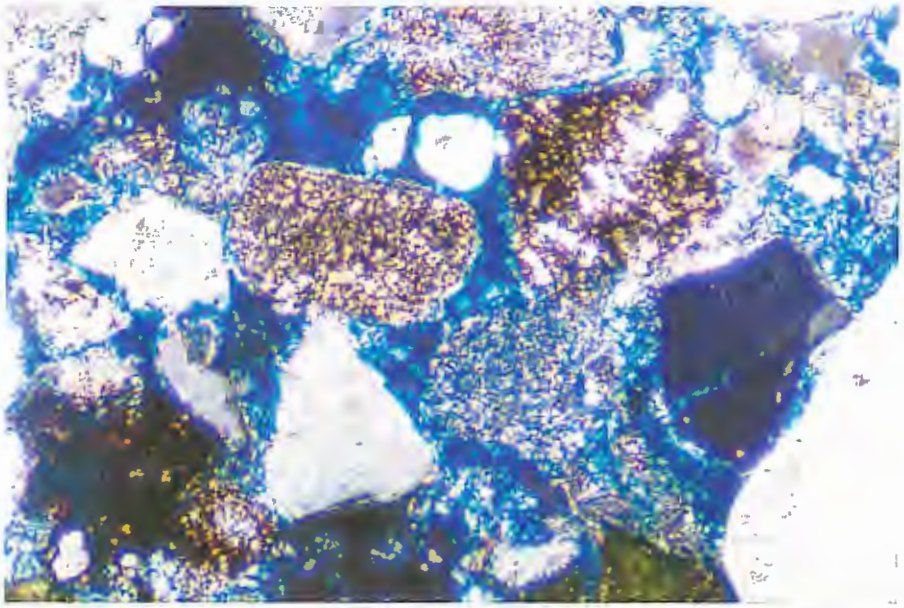

Figure 25. Photomicrograph of various subangular to subrounded chert and quartz grains. Basal sand body of the Lazeart Member, Ms-6, 1m. Crossed-polarized light. Field of view is 1.0 mm wide.

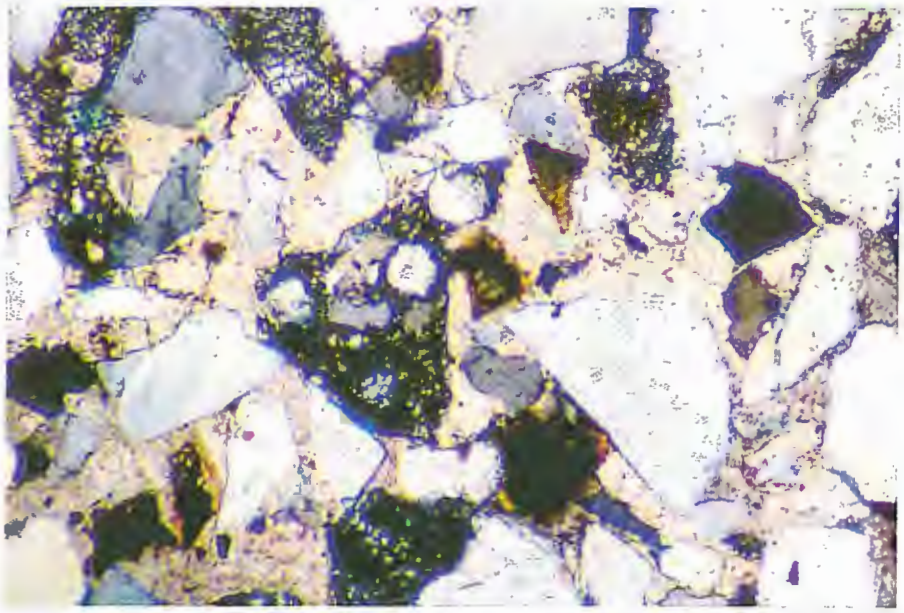

Figure 26. Photomicrograph of a calcite-cemented sandstone containing an felsic volcanic rock fragment (left of center), subangular quartz grains, and chert. Calcite has replaced portions of some chert and quartz grains. Lazeart Member, Ms-1, 43m. Plain light. Field of view is 1.0 mm wide.

sand bodies contain a clay matrix with minor amounts of carbonate cement. As in the Adaville sandstones, minor amounts of quartz cement, chert cement, and vermicular kaolinite cement add bonding strength (Figure 27).

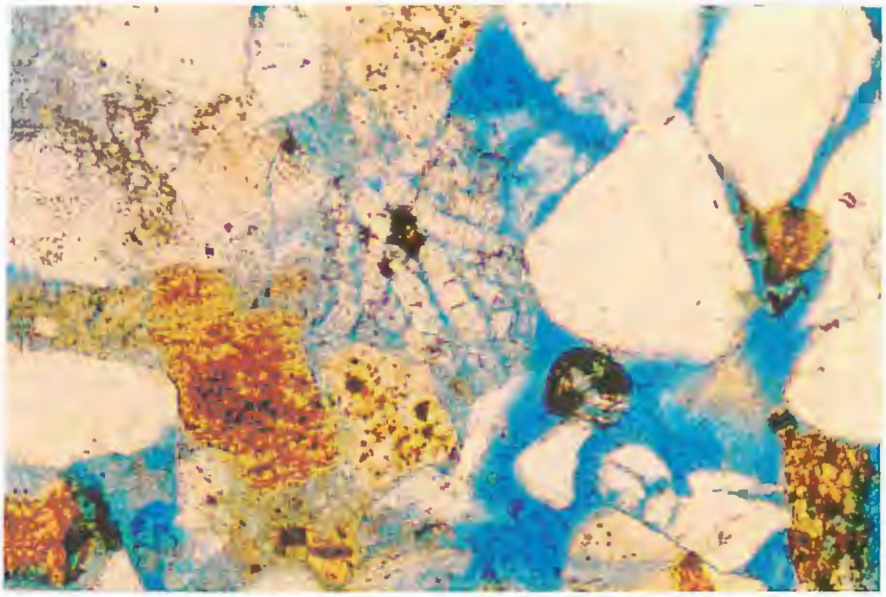

Figure 27. Photomicrograph of vermicular kaolinite (center), chert and quartz grains, and clay matrix. Basal sand body of the Lazeart Member, Ms-1, 6.5 m. Plain light. Field of view is 1.0 mm wide.

Heavy Mineral Analysis

Sample Preparation

Eight representative samples, approximately 8 × 8 × 8 cm, from the Lazeart sand bodies and one from an Adaville sandstone were selected for analysis. Due to the sandstone's poor competence, the samples were split and broken down into an unconsolidated sand fraction with a rubber stopper and pestle. The sand was then placed in a beaker. Distilled water was repeatedly mixed with the sand and drained off to eliminate the clay fraction. The sand was placed in a 150° C oven until dry. Afterwards, the sand was sent through a 0.25 mm sieve to eliminate coarse grains. A binocular microscope was used to make sure that there was no loss of coarse-grained heavy minerals. A sand splitter was used to evenly separate the amount of each bulk sample. Half of the sand fraction from the split sample was weighed. The second half of the sample was retained in case another analysis was needed. Tetrabromoethane, (d=2.95), was used with a separatory funnel to separate the heavy minerals from the light minerals. Each sample was periodically stirred to assist separation. The minerals were cleaned repeatedly with acetone, dried, and weighed. Each heavy mineral fraction was mounted using Canada Balsam. The heavy minerals were systematically identified and counted using a petrographic microscope with a manual point counter.

Samples were labeled according to the measured section (e.g. Ms-1, 6.5 m), core (e.g. c 8669, 41 m), or outcrop that they were taken from. Seven measured sections from Crockers Point represent the Lazeart Member (Figure 3). The measurement appearing after the sample represents the height within the measured section or the depth in a

measured core. A few samples were taken from specific sand bodies within the Lazeart Member without reference to a particular section or height. They are labeled for the sand body they represent (e.g. Lzss unit 1).

Operational Definitions

Apatite

Colorless to yellowish-brown, angular to subrounded grains that have a moderately high relief and low birefringence.

Augite

Dark to light green, subangular grains with extinction between 35 and 45°.

Biotite

Reddish-brown, euhedral to subangular grains.

Epidote

Yellowish green, subangular grains with a high relief, moderate birefringence, and a nearly parallel extinction.

Garnet

Colorless, subangular, isotropic, subrounded grains with a very high relief and isotropic character.

Hypersthene

Pleochroic from pale green to light pink, moderately birefringent, subrounded grains with parallel extinction.

Leucoxene

Opaque rounded to subrounded grains, white to yellowish orange in reflected light.

Pyrite

Opaque, subangular grains, with a metallic brassy luster under reflected light.

Rutile

Yellowish to foxy red, rounded to subrounded grains, with a high relief, extreme birefringence, and parallel extinction.

Tremolite

Colorless to pale green subangular grains, with an inclined extinction angle between 15 and 20°, acicular cleavage, and a weak birefringence.

Tourmaline

Blue, green, pink and yellow rounded to subrounded grains, exhibiting parallel extinction, some pleochrosim, and moderate birefringence.

Zircon

Colorless euhedral to rounded grains, exhibiting high relief, parallel extinction, and high birefringence.

Modal Analysis of Heavy Minerals

The heavy mineral suites of the Adaville Formation and its Lazeart Member are similar (Figures 28 and 29). They commonly contain opaque minerals including leucoxene and pyrite. The non-opaque grain types are dominated by zircon and tourmaline (Table 3). Zircon appears as both euhedral and well-rounded grains (Figures 30 and 31). Rounded zircons make up approximately 41 percent of all non-opaque mineral grains and euhedral zircons make up approximately 25 percent. Pink, green, yellowish-brown, and blue tourmalines are moderately to well-rounded and make up approximately 20 percent of the non-opaque minerals (Figure 32). A few angular tourmaline grains are present. Foxy red to yellow rutile is present (Figure 33); some rutile grains are well-rounded while others are subangular. Minor amount of apatite, epidote, garnet, augite, hypersthene, tremolite, and sphalerite are also present.

The ZTR index (Hubert, 1962) for the Adaville Formation and its Lazeart Member ranges from 76.2 to 92.0. This index is a ratio of zircon plus tourmaline plus rutile to total non-opaque, non-micaceous detrital heavy minerals times one hundred. It is an index of sandstone maturity.

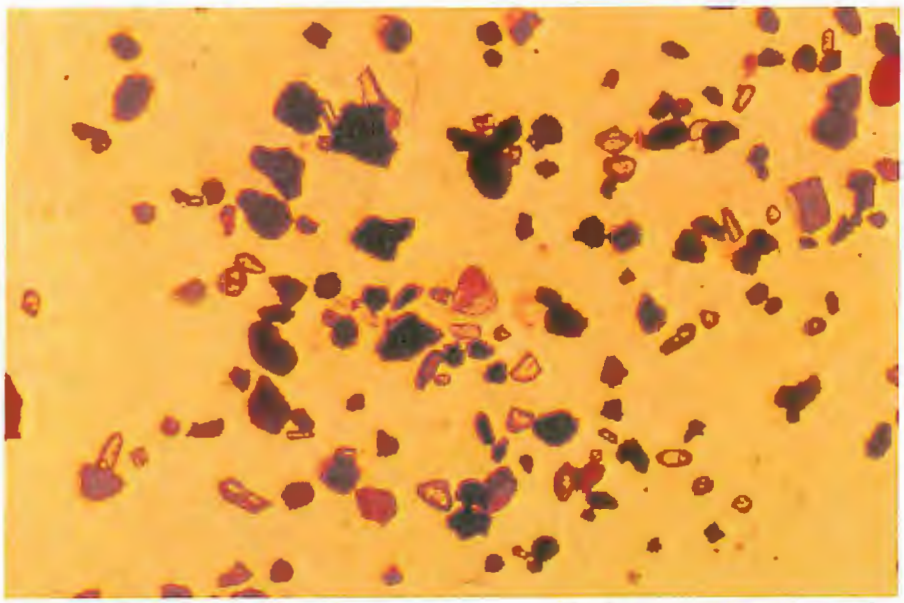

Figure 28. Representative photomicrograph of a heavy mineral suite from the Adaville Formation, core 8669, 41 m. Predominantly zircon, tourmaline, and opaque grains. Plain light. Field of view is 2.5 mm wide.

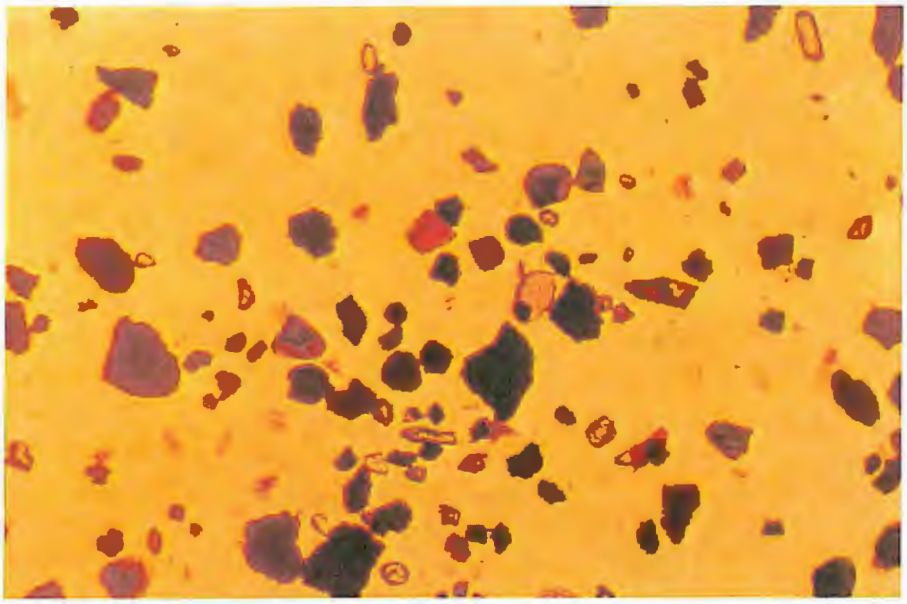

Figure 29. Representative photomicrograph of a heavy mineral suite from the Lazeart Member, Crockers Point sand body 4. Predominantly zircon, tourmaline, and opaque grains. Plain light. Field of view is 2.5 mm wide.

Sample	Adaville, c8669		Lzss unit Two		Ms-1, 6.5m		Ms-2, 18m	
		ZTR %		ZTR %		ZTR %		ZTR %
Zircon, euhedral	98	17.75	20	21.51	54	29.51	22	15.38
Zircon, rounded	248	44.93	47	50.54	72	39.34	45	31.47
Tourmaline, angular	6	1.09	1	1.08	4	2.19	5	3.50
Tourmaline, rounded	108	19.57	7	7.53	21	11.48	46	32.17
Rutile, angular	36	6.52	3	3.23	4	2.76	2	1.40
Rutile, rounded	12	2.17		0.00	6	3.28	6	4.20
ZTR Index		**92.0**		**83.9**		**88.6**		**88.1**
Apatite, angular	17		6		8		4	
Apatite, rounded					4			
Epidote, angular	10		5		7		3	
Epidote, rounded								
Garnet, angular	9				3		4	
Augite	6		1				1	
Hypersthene	2		3				5	
Leucoxene	84		45		48		64	
Biotite			3				1	
Pyrite	23						4	
Other							5	
Total grains counted	659		141		231		217	

Sample	Ms-4, 79m		Ms-10, 80m		Lzss Unit Six		Lzss Unit Four	
		ZTR %		ZTR %		ZTR %		ZTR %
Zircon, euhedral	23	18.85	26	35.14	68	20.24	95	20.52
Zircon, rounded	35	28.69	23	31.08	112	33.33	189	40.82
Tourmaline, angular	4	3.28	1	1.35	7	2.08	13	2.81
Tourmaline, rounded	24	19.67	14	18.92	62	18.45	64	13.82
Rutile, angular	6	4.92	3	4.05		0.00	2	0.43
Rutile, rounded	1	0.82		0.00	38	11.31	53	11.45
ZTR Index		**76.2**		**90.5**		**85.4**		**89.8**
Apatite, angular	10		3		16		7	
Apatite, rounded	1						1	
Epidote, angular	9		1		20		13	
Epidote, rounded								
Garnet, angular	4				4		10	
Starolite								
Augite	2		2		5		8	
Hypersthene	3		1		4		8	
Leucoxene	41		47		89		180	
Biotite	4				3		8	
Pyrite								
Other								
Total grains counted	167		121		428		651	

Table 3. Heavy mineral data sheet showing ZTR percentages of seven sandstone samples from the Lazeart Member (Ms-1, 6.5m; Ms-2, 18m; Ms-4, 79m; Ms-10, 80m; Unit 2; Unit 4; and Unit 6) and one sample from the lower Adaville Formation, (Adaville c8669). (Ms) stands for measured section and (c) stands for core. Each sample has a thin section as well.

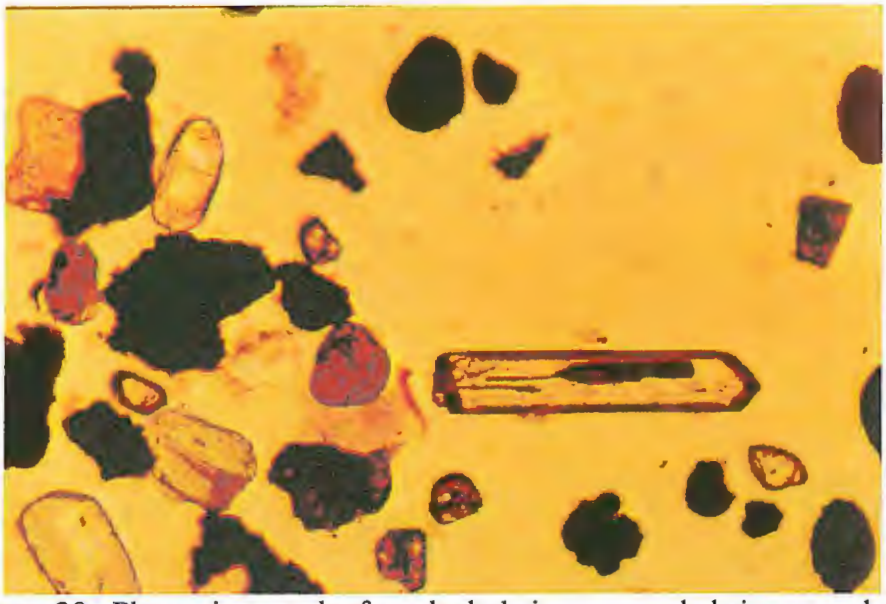

Figure 30. Photomicrograph of a euhedral zircon, rounded zircons and rutile (left of center). Adaville Formation, core 8669, 41m. Plain light. Field of view is 1.0 mm wide.

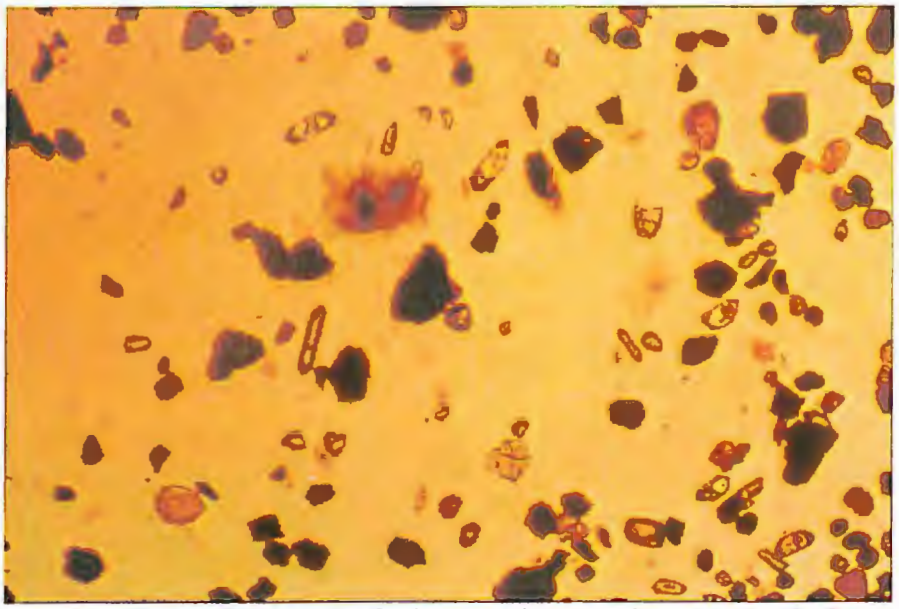

Figure 31. Photomicrograph of a heavy mineral suite composed of rounded and euhedral zircon, rounded tourmaline and opaque leucoxene. Lazeart Member, Sp-1, 110 m. Plain light. Field of view is 2.5 mm wide.

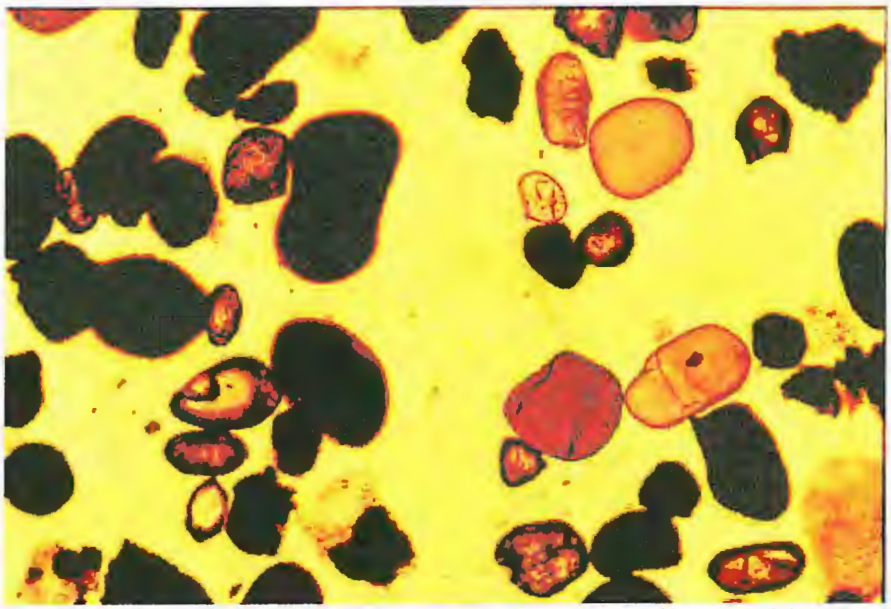

Figure 32. Photomicrograph of rounded tourmaline, zircon, epidote, and opaque grains. Adaville Formation, core 8669, 41m. Plain light. Field of view is 1.0 mm wide.

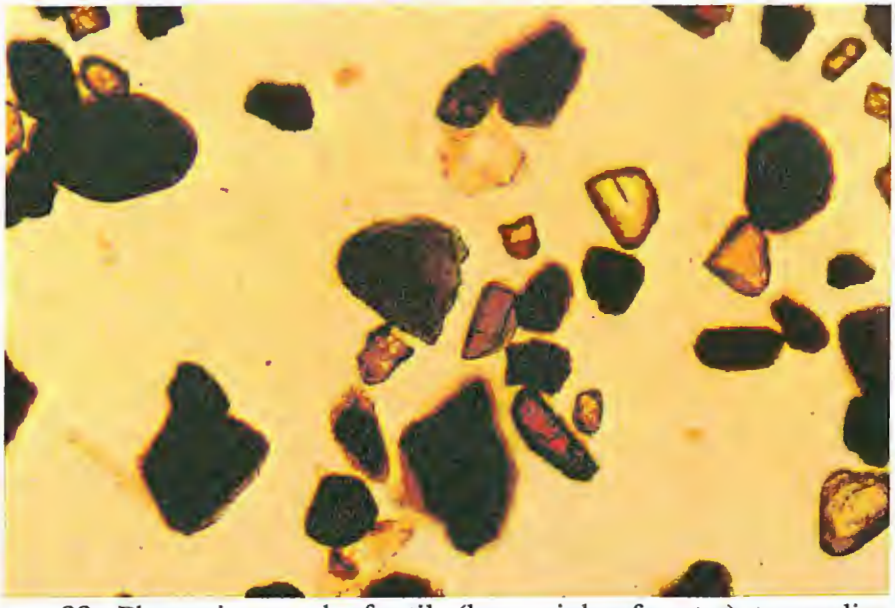

Figure 33. Photomicrograph of rutile (lower right of center), tourmaline, zircon, and hypersthene (center). Lazeart Member, Crockers Point sand body 4. Plain light. Field of view is 1.0 mm wide.

X-Ray Diffraction Analysis

While studying the Adaville Formation, it became apparent that clay mineralogy is an important factor because the Lazeart Member contains a significant amount of clay. X-ray diffraction was used to aid in elemental analysis and subsequent clay identification. I chose ten representative samples from the Adaville Formation for analysis. Each sample was crushed into a powder and added to a 200-ml beaker. While mixing, I added distilled water to separate the clay particles. I used a pipette to extract clay particles from solution and allowed the labeled glass plate to air-dry. To prevent contamination, distilled water was used.

I analyzed the samples using a Philips Analytical Diffractometer at the University of Minnesota-Duluth. The diffractometer contains a Cu K-alpha X-ray tube, and the rays were Ni-filtered. The focusing tube slit was set at one degree with the detector slit at a width of 0.4 mm. Most sampling procedures took approximately twenty-seven minutes while the machine ran at 45 kV and 18 ma. The diffractometer measured from two degrees 2-theta to thirty degrees 2-theta. This range will present the (001) reflections of minerals within the Adaville Formation. X'pert Graphics software produced diffractograms that were used to assist mineral verification.

X-ray diffraction analysis is based on the fact that crystals with different compositions have different atomic spacing values. In addition, distinct θ values should yield unique wavelength patterns. Software settings automatically standardized each diffractogram for any goniometer zero-alignment problems. The standard for verifying correct alignment is quartz. Quartz grains are small enough to be present within the clay-

size fraction. The crystalline nature of quartz is not susceptible to atomic substitution at the peak levels of (100) and (101). The peaks appear on each diffractogram at 20.85° (2θ) and 26.65 (2θ). The software calculated the d-spacing of each peak using Bragg's law: $2d (\sin\theta) = n(\lambda)$, where d is the distance between layers of crystal atoms (in A); θ represents the reflected angle of the X-ray beam; and n (λ) is the number of integral wavelengths of the incident X-ray (in A).

Kaolinite is common. Diffractograms exhibit strong kaolinite peaks at (001) and (002). The peaks occur at 12.5 (2θ) at 7.16 A and 24.9 (2θ) at 3.58 A, respectively, for air-dried samples. Moore and Reynolds (1997) showed that kaolinite is amorphous and will loose its peak intensity upon heating. The samples were placed in a 600° C oven for one hour, cooled, and analyzed. The result was a disappearance of the representative kaolinite (001) and (002) peaks. The (060) reflection measured 1.49 A.

Minor illite appears in all samples of the Adaville Formation and in its Lazeart Member. Non-treated illite forms sharp low-intensity peaks at 10.1 A and approximately 8.85° (2θ). Quartz and carbonate reflections made it difficult to ascertain possible illite polymorphs. Mixed layers of illite and smectite are present within some of the Lazeart sandstones and interbedded shales. The mixed layer clays form broad peaks that are centered on 6.5° (2θ) in air-dried samples. Heating the samples at 550° C for one hour dehydrated the smectite and left the illite peak.

An analyzed concretion within the Lazeart Member contained kaolinite, quartz, and calcite. The calcite is evident due to its very intense sharp peak at 29.43° (2θ) and 3.86 A. Diffractograms exhibited the presence of feldspar within each sandstone of the

Lazeart Member. The feldspar peaks are sharp and occur approximately at 27.5° (2θ) and 3.24 A. Such peaks are representative of the K-feldspars, (monoclinic) orthoclase and (triclinic) microcline (Moore and Reynolds, 1997). Coupled with petrographic observations, the dominant feldspar within the Lazeart Member is orthoclase. Microcline is present in lesser amounts.

SEM Analysis

While studying thin sections and X-ray diffraction data from the Adaville Formation, it was necessary to use a scanning electron microscope, SEM, for the following reasons: to accurately determine clay mineralogy, gain further insight regarding diagenesis, and distinguish authigenic kaolinite, quartz, and K-feldspar grains from detrital grains. An EDS, energy dispersive system, aided in the project's elemental verification and analysis. I used a Hitachi S-150 SEM with a Kevex 8um window EDS detector at the University of Wisconsin Eau-Claire.

I chose ten representative samples from the Adaville Formation. The samples consist of six Lazeart sandstones, two Adaville siltstones, an interbedded shale between Lazeart sand bodies, and an unknown white layer from the Adaville Formation. Each sample was oven-dried at approximately 250° C overnight and then split to reveal a fresh surface. From the fresh surface, a small piece was cleaved off using an X-acto blade. A portion of this piece was placed on a specimen plug using double-sided tape. To obtain a clear image, samples were coated with gold using argon gas. Next the samples were analyzed with the SEM. The accelerating voltage setting ranged from 15 to 20 KV. Photographs were taken at a magnification of 2,000 to 25,000 ×, using a 4 × 5 Polaroid camera.

The SEM beautifully captures information and images from the sandstones within Lazeart Member. The data verify the presence of silica cement, authigenic quartz overgrowths, vermicular kaolinite, diagenetic alteration of potassium feldspar to kaolinite, and dissolved orthoclase (Figures 34 to 40). The Lazeart Member has

interbedded layers of silty shale that contain framboidal pyrite, kaolinite, illite, and pollen (Figure 41).

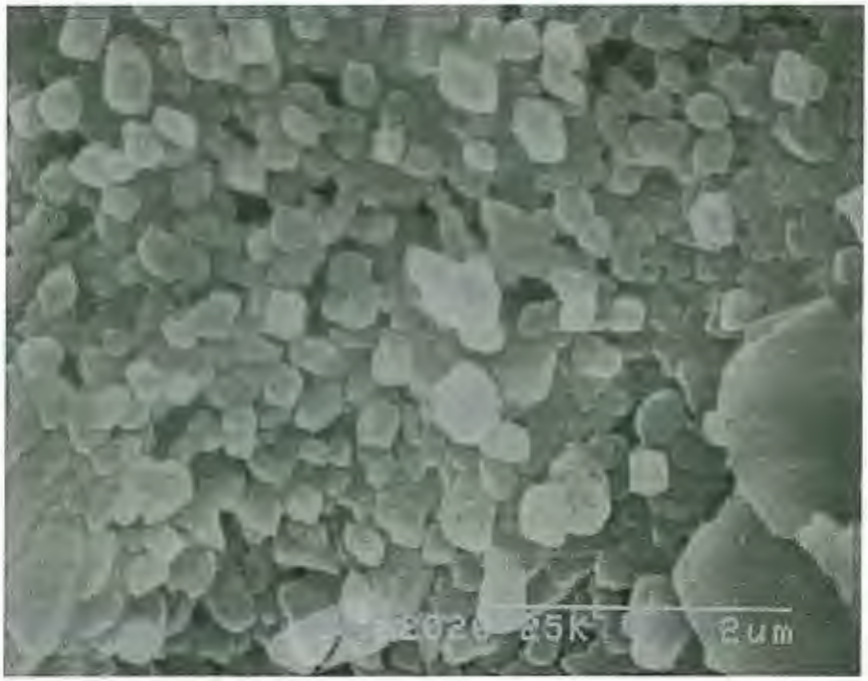

Figure 34. SEM photomicrograph of silica cement and kaolinite flakes (bottom right). The photo is from the Lazeart Member, Ms-1, 6.5 m. Note the bar scale of this photo it is only 2 um.

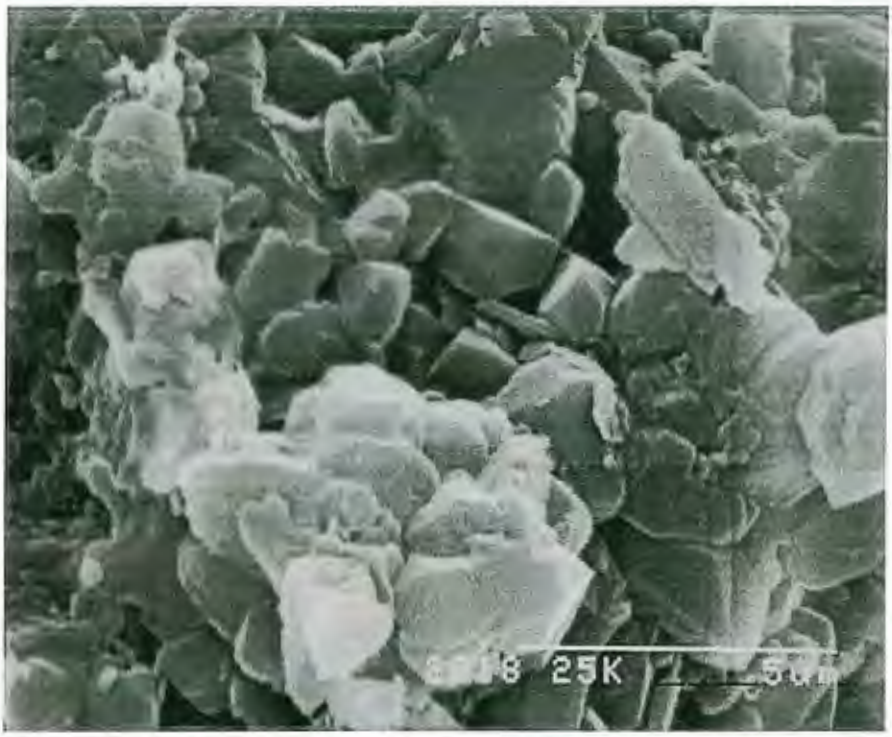

Figure 35. SEM photomicrograph of pore-filling quartz overgrowths. The photo is from a sandstone in the Lazeart Member, Ms-1, 6.5 m.

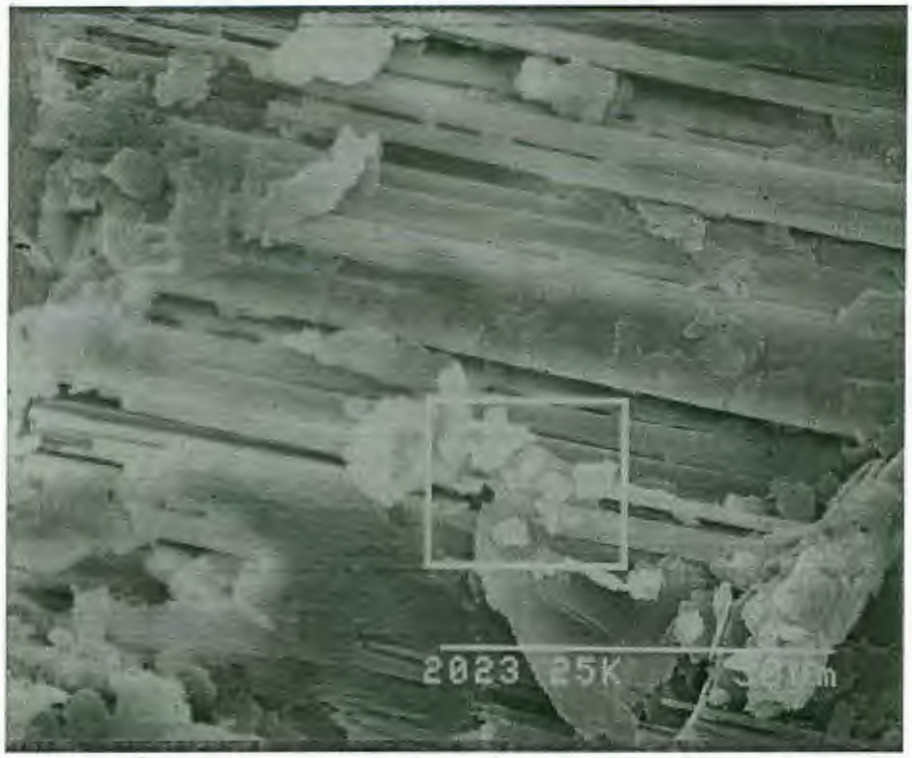

Figure 36. SEM photomicrograph of an orthoclase grain exhibiting well-defined cleavage and alteration to kaolinite. Basal Lazeart Member, Ms-1, 6.5m.

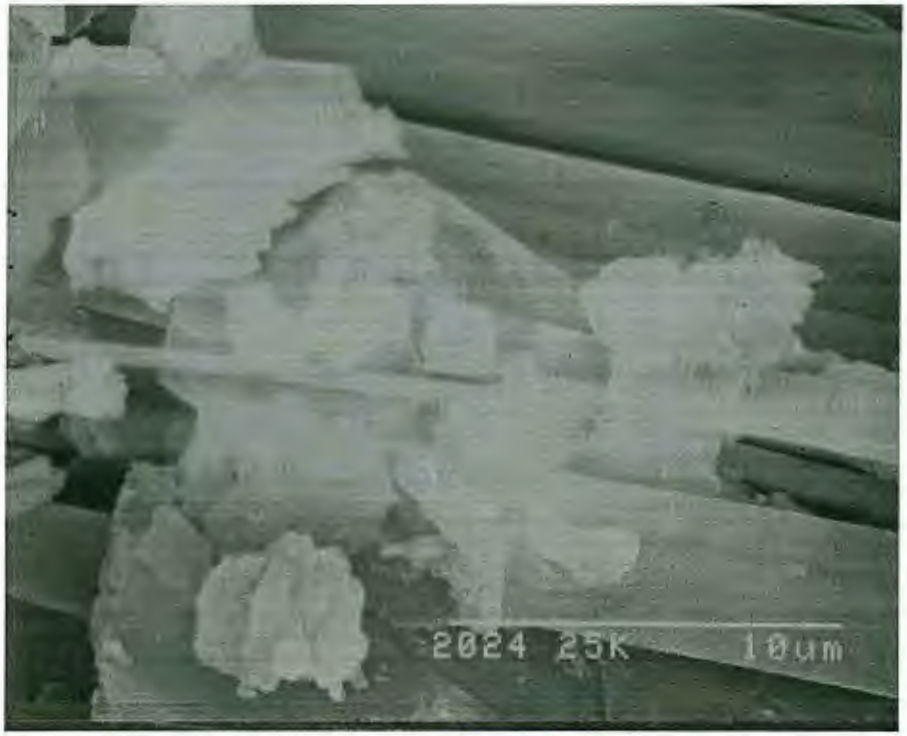

Figure 37. SEM photomicrograph, a closeup of previous figure showing alteration of orthoclase to kaolinite.

Figure 38. SEM photomicrograph of vermicular kaolinite forming delicate book structures. Lazeart Member, Ms-1, 6.5 m.

Figure 39. SEM photomicrograph of vermicular kaolinite. Lazeart Member, Ms-1, 6.5 m.

Figure 40. SEM photomicrograph of an altered orthoclase grain surrounded by kaolinite flakes. Lazeart Member, Ms-1, 6.5 m.

Figure 41. SEM photomicrograph of framboidal pyrite (left of center), kaolinite, smectite (elongate filaments). The sample is an interbedded shale between sand bodies of the Lazeart Member.

Diagenesis

Identified authigenic minerals include hematite, pyrite, quartz, and kaolinite. Pyrite and hematite locally occur within the Adaville Formation. Pyrite is typically well-crystallized. Hematite occurs as massive cement. Quartz overgrowths constitute 1.80 and 2.22 percent of the Adaville Formation and the Lazeart Member respectively. Scanning electron images and thin sections of Lazeart quartz grains show euhedral overgrowths (Figure 34). As quartz overgrowths increase, the amount of feldspar typically decreases. The diagenetic processes of dissolution of feldspar and hydrolysis are a probable cause for this general trend.

Carbonate cement, mainly calcite, is present within localized sand bodies of the Lazeart Member, especially in sandstone number two (Figure 2). Where carbonate cement is present, it typically makes up nearly 20 to 50 percent of the thin section. Carbonate cement greatly reduces the amount of chert and quartz, as it has replaced the silica (Figure 25).

The dominant pore-filling substance is a mixture of detrital and authigenic clay matrix. Common clay types within the Lazeart Member are illite, kaolinite, and trace amounts of smectite. Clay matrix makes up approximately fourteen and eleven percent of the Adaville Formation and its Lazeart Member respectively. Kaolinite is the dominant clay type within the Adaville Formation and Lazeart Member. It often takes on a vermicular form, exhibiting well-developed book structures. Such delicate structures are unlikely to be present in detrital clay. Thus, vermicular kaolinite is thought to be authigenic. Authigenic kaolinite forms by the partial dissolution of feldspar and other

clay minerals. As the solid feldspar dissolves and reacts with the surrounding water, the solid phase of the feldspar and solute is altered. An example of alteration from partial dissolution is the kaolinization of K-feldspar. This hydrolysis reaction identifies K+, H_4SiO_4, and H+ as dissolved aqueous species that are important variables of the kaolinization of K-feldspar:

$$2KAlSi_3O_8 + 2H^+ + 2(HCO_3^-) + 9H_2O \leftrightarrow Al_2Si_2O_5(OH)_4 + 4H_4SiO_4 + 2K^+ + 2HCO_3^-$$

The aluminum is retained in the aluminosilicate structure and does not enter solution. If the activity of K+/H+ falls below five or six and the H_4SiO_4 concentrations drop to 10^{-3} moles per liter, kaolinitization of K-feldspar will occur (Pettijohn et. al., 1987, p. 440).

The Lazeart Member exhibits extensive kaolinization of K-feldspar. Petrographic, scanning electron microscopic, and electron dispersion analysis verify the transformation of K-feldspar to kaolinite (Figures 37 and 38). Vermicular kaolinite makes up as much as 5.7 percent of the whole rock and averages 1.2 percent within the analyzed sandstones of the Lazeart. Diagenesis may help to describe the depositional environment of the Lazeart Member. For kaolinization of K-feldspar to occur, the local groundwater must contain low amounts of K+, H_4SiO_4, and dissolved solids and have a neutral pH level. Meteoric water and atmosphere interactive systems such as nearshore environments contain the chemical characteristics needed for kaolinization.

Sandstone porosity within the Lazeart Member ranges from approximately 0 to 24 percent. The average porosity is 12.6 percent. Samples with a porosity of less than four percent are carbonate-cemented. Silica overgrowths significantly reduce porosity. Minor compaction of a soft clay matrix also may lessen the porosity. Authigenic vermicular

kaolinite as diagenetic cement may further decrease porosity. Minor secondary porosity occurs through the process of dissolution of feldspar grains in the Lazeart Member. The porosity of the Adaville Formation ranges from 0 to 17 percent and averaged 6.3 percent for five thin sections. Porosity may be increased by dissolution and fractures caused by faulting (Pettijohn et. al., 1987, p. 464).

The Cenomanian and Turonian sandstones of the Frontier Formation are depositionally and diagenetically similar to the sandstones of this study. Dutton's (1993) petrographic study reveals the major diagenetic events within the sandstones of the wave-dominated deltaic Frontier Formation as: mechanical compaction by grain rearrangement and deformation of ductile grains, formation of illlite and mixed-layer illite-smectite rims, precipitation of quartz overgrowths, calcite, and kaolinite cement, and the dissolution of feldspar, chert, biotite, mudstone grains, and calcite cement. The Adaville and Frontier formations have similar depositional settings, provenance, tectonic settings, and diagenesis.

PROVENANCE

Introduction

Studying provenance gives geologists an opportunity to learn about the paleogeographic origin of sediment. Provenance may answer such questions as the original source rock type, the climate during deposition, and the length of sediment travel. Sandstones are the best indicators of provenance. Indicators of provenance within sandstones are types of detrital quartz grains, feldspars, rock particles, heavy mineral assemblages, and abundance of mica. Provenance interpretation may be problematic due to physical and chemical variations in mineral solubility and the fact that most sandstones are recycled. Multiple source areas, differential weathering, and diagenesis further complicate the analysis of provenance. The Lazeart Member and sandstones of the Adaville Formation were studied to ascertain the provenance of the original sands.

Petrographic Interpretation

Detrital Quartz

The dominance of undulose quartz grains and polycrystalline (i.e. metamorphic) grains within the Lazeart Member suggests a tectonically active source area. A high ratio of undulose to non-undulose quartz indicates a deformed igneous to metamorphic terrain. The ratio of undulose to non-undulose quartz grains in the Adaville sandstones is 14:1, and in the Lazeart Member it is 10:1. Such ratios indicate a deformed metamorphic - plutonic source area.

Studies by Young (1976) show that polycrystalline quartz may also indicate a metamorphic or igneous source area, depending on grain characteristics. Furthermore, the ratio of polycrystalline to monocrystalline quartz appears to be a maturity index and possible source area indicator (Pettijohn et. al., 1987, p. 256). The poly- to monocrystalline ratio for the Adaville Formation is 1:30. The Lazeart Member's ratio is 1:20. Potter and Pryor (1961) have shown that a high ratio of poly- to monocrystalline quartz, especially on the North American Craton, may indicate a tectonic source area. Such low ratios for the Adaville Formation and its Lazeart Member may be a function of weathering, diagenesis, and a high-energy wave-dominated coast. The chemical and physical action of such natural forces work to eliminate polycrystalline quartz grains.

Feldspar and Mica Content

Detrital unaltered orthoclase is the dominant feldspar within the Adaville Formation and the Lazeart Member. The feldspar ratio in the Qm:F:Lt index for each sandstone is approximately ten, classifying the sandstones as feldspathic. The presence of orthoclase and microcline suggests an acidic plutonic rock source. The effects of diagenesis, weathering, and the general instability of feldspars complicate provenance interpretation. A substantial K-feldspar abundance (5 percent) and the presence of biotite within the Adaville Formation indicate a proximal source area.

Rock Particles

Rock particles within sandstone are excellent clues to provenance. The main particle types found in the sandstones of the Lazeart Member are chert, polycrystalline

quartz, metamorphic, and plutonic K-Q fragments. Cretaceous sands of Wyoming and Colorado commonly contain chert particles. Chert particles are also common in lithic arenite deposits produced from a source area of carbonate rocks. If such an area has a low to moderate relief and an humid climate, the chert would be derived from replacement chert nodules and beds.

Pryor's (1961) petrographic study of the Upper Cretaceous Mesaverde Group of Wyoming included one sample of the Adaville Formation. Pryor noted a significant decrease in chert percentages eastward. The polycrystalline habit of chert typically leads to disintegration during transport. Therefore, a western provenance characterized by increased amounts of chert towards the source area is probable. Pryor suggested that a likely parent rock for chert-rich sandstones in the Mesaverde Group is the Rex Member of the Lower Permian Phosphoria Formation. This seems applicable to the Adaville Formation and its Lazeart Member as well. The Sevier Orogeny initiated the expansive Absaroka Thrust system that brought several sedimentary deposits including the Phosphoria Formation to the surface.

The Lazeart Member also contains plutonic rock fragments from the orogenic highlands to the west. The presence of fresh K-feldspar, rock fragments containing plutonic K-feldspar and quartz, and metamorphic fragments may link the Lazeart sands to the Idaho batholith. Rivers carried weathered detritus from the Idaho batholith eastward into the Cretaceous foreland basin and the Lazeart wave-dominated deltaic system. Some of the Idaho batholith's rock types are pelitic schist, calc-silicate gneiss, and quartzite (Hyndman, 1984). Granitic intrusions into the batholith are weakly foliated, medium-grained, micaceous, and with K-feldspar megacrysts (Bickford et. al., 1981). The

proximity and composition of the Idaho batholith make it a likely source area for the Adaville sandstones.

Heavy Minerals

Heavy minerals are useful in provenance determination because certain assemblages are characteristic of particular source areas. Current research on the Amazon River sediment exhibits the importance of heavy minerals in provenance determination (Vital et. al. 1999). Heavy mineral analysis of the Adaville Formation and its Lazeart Member identified zircon, tourmaline, rutile, apatite, epidote, garnet, augite, hypersthene, leucoxene, pyrite, and tremolite. The probability of multiple source areas became evident with the identification of both rounded and euhedral specimens of zircon and tourmaline. The identified heavy mineral associations may correlate with acid igneous rocks, basic igneous rocks, and reworked sediments (Table 4). This association further indicates that the source areas for the Lazeart sands were the sedimentary Paleozoic rocks of the fold-and-thrust belt and the orogenic highland detritus of the Idaho batholith.

Source	Association
Acid igneous rocks	Apatite, biotite, hornblende, monazite, muscovite, rutile, titanite, tourmaline (pink), zircon
Granite pegmatites	Cassiterite, dumortierite, fluorite, garnet, monazite, muscovite, topaz, tourmaline (blue), wolframite, xenotime
Basic igneous rocks	Augite, chromite, diopside, hypersthene, ilmenite, magnetite, olivine, picotite, pleonaste
Contact meta/ rocks	Andalusite, chondrodite, corundum, garnet, phlogopite, staurolite, topaz, vesuvianite, wollastonite, zoisite
Reworked sediments	Barite, iron ores, leucoxene, rutile (rounded), tourmaline (rounded), zircon (rounded)

Table 4. Heavy mineral associations and provenance (Modified from Feo-Codecideo,1956).

Provenance and Tectonic Setting

Dickinson et. al. (1983) proposed that triangular QFL and QmFLt compositional diagrams may be subdivided into three provenance terranes that are specified by plate tectonics. The main terrane types are recycled orogens, magmatic arcs, and continental blocks (Figure 42). Using this system, the Adaville and Lazeart sandstones are categorized as recycled orogen sediments. The definition of a recycled orogen is a sedimentary sequence that may be partially metamorphosed and is exposed by the orogenic uplift of fold-and-thrust sheets and are commonly low in feldspar (Dickinson et. al., 1983). The Lazeart sandstones fit moderately well into this classification, with the abundance of recycled sedimentary grains. The Lazeart's feldspar content is interpreted to reflect its proximity to the Idaho batholith.

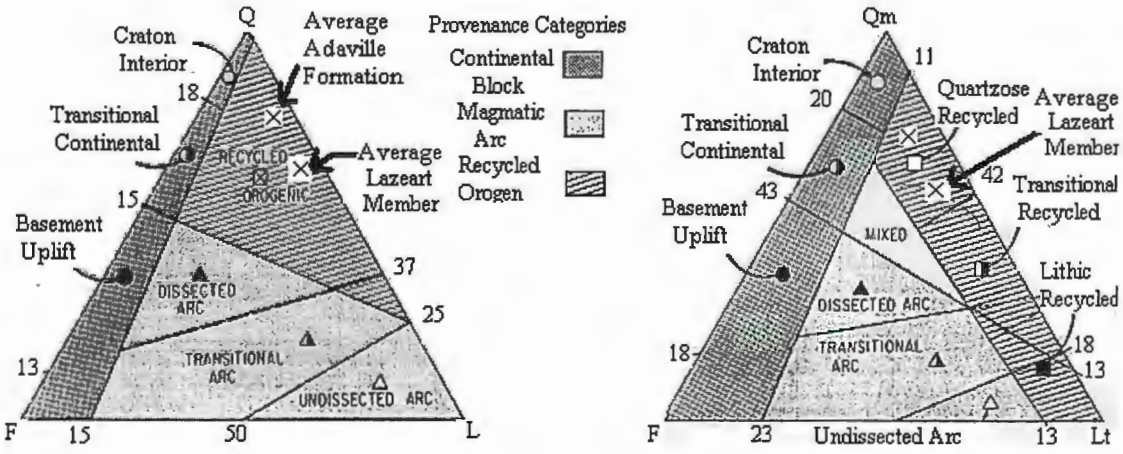

Figure 42. QFL ternary diagrams exhibiting the relationship between sandstone composition and tectonic setting of the Adaville Formation and its Lazeart Member. (After Dickinson et. al., 1983).

Provenance Summary

1. High percentages of dark chert grains give Lazeart sandstones a "salt and pepper" appearance.

2. Lazeart chert fragments are predominantly recycled from Paleozoic sedimentary deposits that were exposed during movement of the Absaroka Thrust Fault system. Specifically, the chert probably came from the Rex Member of the Permian Phosphoria Formation. The Mississippian Madison Formation may be an additional chert source.

3. At least two source areas supplied detritus to the Lazeart wave-dominated complex throughout its history. Elevated Paleozoic strata supplied recycled sedimentary deposits to the basin. The Cordilleran Highlands, including the Idaho batholith, contributed both plutonic and metamorphic detritus.

4. The presence of euhedral and rounded zircon and tourmaline help to identify two source areas. Rounded minerals are interpreted to have been derived from the recycling of Paleozoic strata, and euhedral minerals are interpreted to have been derived from the crystalline Idaho batholith.

5. The abundance of chert and the presence of unstable heavy minerals such as hypersthene and augite suggest a proximal source area.

PALEOCURRENT ANALYSIS

A total of 107 paleocurrent measurements taken from channels and cross-bedding make up the database for this study. Trough cross-bedding within the Lazeart Member at Crockers Point provided approximately eighty-five percent of the database. I used a Brunton compass to record master beds, cross-bedding, and location of each measurement. Such measurements may give insight to ancient directional flow patterns after correction for post-depositional tilt (Phillips, 1954).

Previously classified as a marginal marine nearshore sandstone (Lawrence, 1984), the Lazeart Member serves as an excellent source for paleocurrent data. At Crockers Point, five Lazeart sand bodies are successively interbedded with reddish-brown silty shale. The basal sandstone conformably overlies the Hilliard Shale, and contains trough cross-beds and rare herringbone cross-beds. Cross-bedding becomes less common upward except for the sixth and final Lazeart sand body. Past research suggests the Lazeart wave-dominated delta's progradational trends were southeastward throughout its depositional history (Lawrence, 1984).

Measurements collected for this study reaffirm a general southeast progradational trend. The rose diagrams (Figures 43 and 44) show bimodal to polymodal plots. Lazeart Member sand bodies one and three (Figure 2) are bimodal. Sand bodies two and six are polymodal. Sand bodies four and five do not contain obvious cross-beds. Sandstones within the Adaville Formation have polymodal measurements. Although all diagrams are either polymodal or bimodal, each also exhibits a strong southeastward trend.

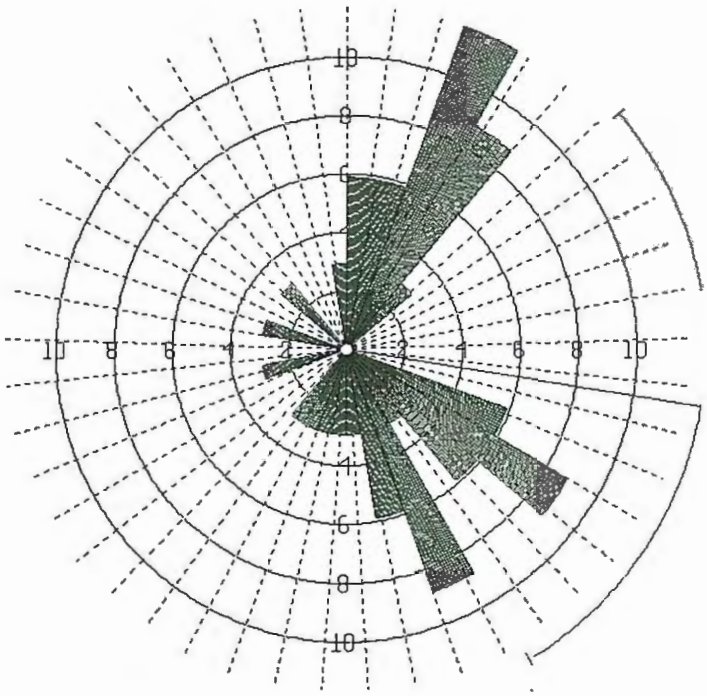

Lazeart Member basal sandstone from Crockers Point, (N=34).

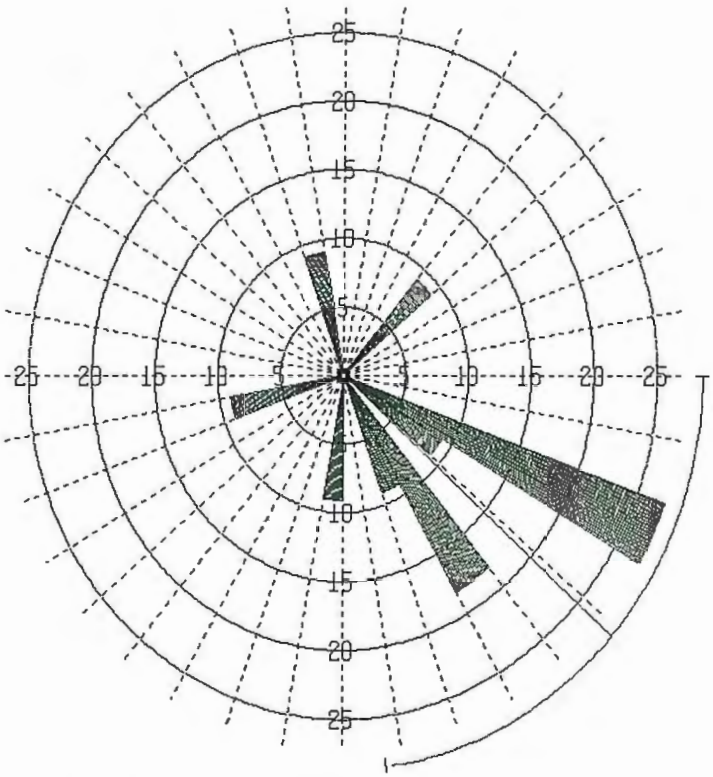

Lazeart Member second sandbody from Crockers Point, (N=11).

Figure 43. Rose diagrams showing Lazeart Member paleocurrent directions.

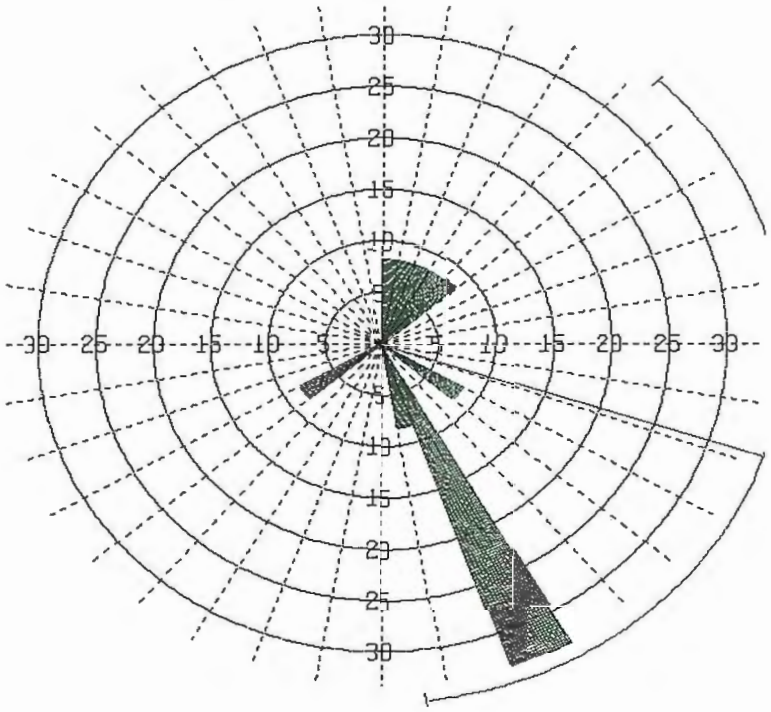

Lazeart Member third sandbody from Crockers Point, (N=12).

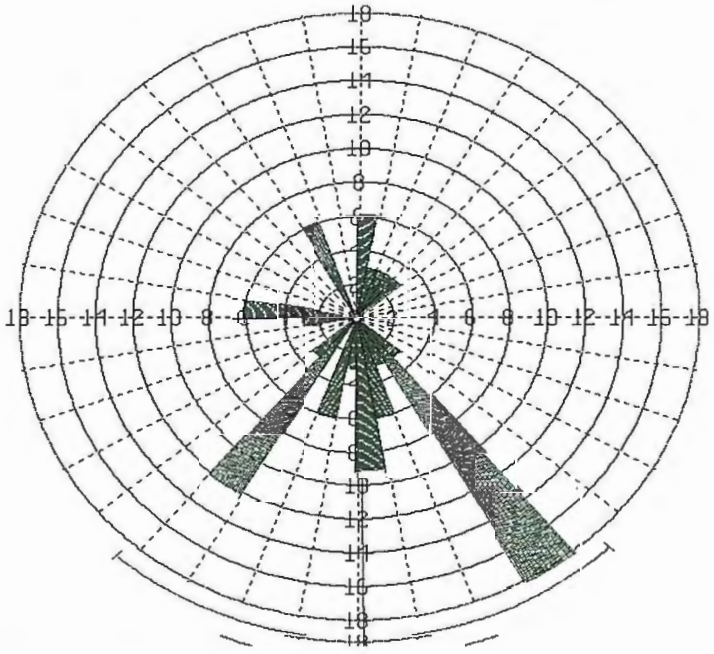

Lazeart Member from the sixth sandbody at Crockers Point, (N=34).

Figure 44. Rose diagrams showing Lazeart Member paleocurrent directions.

ENVIRONMENT OF DEPOSITION

Introduction

Understanding sedimentary depositional environments is of vital importance to a geologist. The stratigraphic record is essentially an open book that contains the history of Earth. From this record we have the opportunity to learn about global climate changes, potential economic reserves, and the biological evolution of the planet. By studying the Adaville Formation, its Lazeart Member, and others like them, we may acquire such knowledge. Veatch (1907), Lawrence (1984), and others have classified this study area as the Lazeart wave-dominated deltaic complex.

Deltas

Deltas are "discrete shoreline protuberances formed where rivers enter oceans, semi-enclosed seas, lakes or barrier-sheltered lagoons and supply sediment more rapidly than it can be redistributed by indigenous basinal processes" (Elliott, 1981, p. 97). Galloway (1975) recognized that delta morphology is controlled by the relative dominance of three basinal processes: river, wave, and or tidal energies (Figure 45). Combining such processes with other autocyclic and allocyclic factors such as sediment size and composition, climate, basin salinity, size and shape of the receiving basin as a function of tectonism, and eustasy interacting at varying degrees of strength throughout time, produces a complex depositional system.

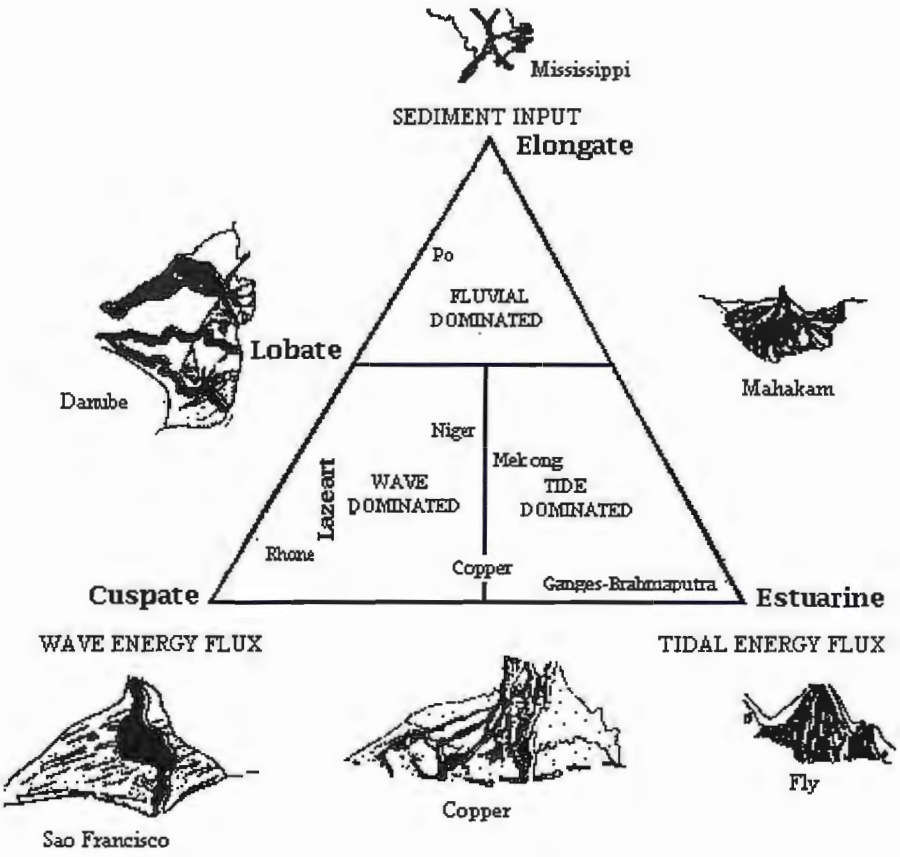

Figure 45. Triangular process classification of deltaic depositional systems. (After Galloway, 1975).

Morphologically, a delta consists of a delta plain, delta front, prodelta, and numerous sub-environments. The delta plain correlates with the main coal-bearing body of the Adaville Formation. Delta plains are transitional lowland areas that host distributary channels, bays, marshes, swamps, lakes, tidal flats, floodplains, and are hypersensitive to environmental change. Sedimentary deposits are primarily based upon the sub-environment characteristics. Typically, deltaic plain sediments range from

mudstone to siltstone with occasional interbedded sandstone. Sediments are locally reworked by bioturbation and commonly contain organic debris. Delta plains also serve as a substrate for the accumulation of substantial organic matter deposits during periods of regression.

The delta front occurs at the interaction point between fluvial dispersion and basinal processes. The Lazeart Member correlates with a delta front facies. As sediment enters the receiving basin by fluvial processes, competence is lost due to increased area and decreased velocity. Consequently, the sediment load is released and becomes subject to basinal process such as waves, tides, longshore drift, and ocean currents (Elliott, 1981). The initial distance that sediment may travel upon entering a basin depends on the interactive densities between the channel outflow and basin water. Commonly when fluvial water mixes with basin saltwater, hypopycnal flow occurs. The density of the fluvial water combined with its bed load is typically less than saltwater. This creates a buoyant sediment plume that is carried basinward. A wave active or tidally active environment would negate such hypopycnal flow. Delta front sediment commonly is comprised of silt- and sand-sized particles, coarser than delta plain deposits.

Basinal processes dominate the formation of the prodelta. The finest mud and silt particles introduced into the receiving basin settle out of suspension. Prodelta deposits are relatively thick when compared to the deltaic plain and front. For instance, the prodeltaic Hilliard Shale is approximately 1,800 m thick. In comparison, the combined thickness of the Lazeart wave-dominated complex's deltaic plain and front is only 800 m. Prodeltaic deposits are commonly bioturbated.

Deltaic Classification

Fluvial-Dominated Deltas

Frequent channel migration and subsequent delta lobe changes characterize fluvial deltas. Basinal processes (wave and tidal energy) are absent to ineffective methods of distributing sediment in this type of delta. The lack of basinal sediment redistribution creates a damming effect at the end of each fluvial channel by the buildup of mud, silt, and sand, forcing the channel to change direction and release its load. Fluvial deltas typically form elongate to lobate delta plains that parallel depositing rivers. Common sub-environments within a fluvial-dominated delta are point bars, abandoned distributaries, cravasse splays, and braided steams. A classic modern analog is the Mississippi Delta.

Tide-Dominated Deltas

Tide delta morphology is characterized by three sub-environments with different tidal ranges: microtidal (< 2m), mesotidal (2-4 m), and macrotidal (>4 m). There are two types of tide-dominated deltas: those with an indented coastline or estuary due to very strong tidal currents and those that gradually prograde irregularly basinward and contain tidal channel distributaries. Tidal distributary channels are typically sinuous to straight flaring systems that deposit variable lithologies parallel to depositional slope.

Hayes (1975) described the characteristics of micro-, meso-, and macrotidal deltas as follows:

(1) Microtidal: Tidal range is less than two meters, deltas are small, are formed largely by storms, and are subordinate to wave-formed coastal barriers,

beaches, and river deltas. Dominant transport processes are wind and waves rather than tides.

(2) Mesotidal: Tidal range is two to four meters, principle sandbodies are large tidal deltas that are either flood deltas deposited inward of a coastal barrier or ebb deltas deposited seaward of the tidal inlets. Barrier islands short and stubby. Meandering tidal channels with point bars behind barriers. Dominant transport processes are tides.

(3) Macrotidal: Tides exceed four meters and are the overwhelming transport process. Linear sandbodies, perpendicular to depositional strike parallel tidal currents in a broad funnel-shaped estuary, whose shore may have wide muddy tidal flats. Examples of modern tide-dominated deltas include the Fraser and Mahakham Deltas.

Wave-Dominated Deltas

Wave-dominated deltas are formed on coasts where wave action causes substantial sediment transport and predominates over the effects of tides (Heward, 1981). Dominant storm-driven waves aggressively rework incoming sediment and tend to form laterally extensive arcuate deltas. Wave-dominated deltas tend to form coarsening-upward sequences through successive facies. Also, the prodelta muds are typically thinner, sandier, and more bioturbated than fluvially dominated muds. The deltaic framework often contains a coastal barrier, beach-ridge sands, and frequent dunes that are deposited parallel to depositional strike. Examples of wave-dominated deltas preserved in the stratigraphic record are the Upper Cretaceous San Miguel Formation (Weise, 1980) of Texas and the Dunvegan Formation (Bhattacharya and Walker, 1991) in northwestern

Alberta. Examples of modern wave-dominated deltas are the Rhone, Tiber, Nile, and Sao Francisco.

Lazeart Wave-Dominated System

In order to classify a depositional setting as deltaic, it must meet a certain set of criteria. Beyond the required transitional, terrestrial-marine environment, the point source for sandy deposits must be derived from distributary channels and mouth bars. Also differentiating prograding wave-dominated deltas from strandplains or barrier island systems requires good three-dimensional facies analysis (Bhattacharya and Walker, 1992). Lawrence (1984) determined that at least six of the nine mappable Lazeart sandstone bodies developed by minor transgressive-regressive pulses are of a deltaic nature for the following reasons:

1. Distributary channels or mouth bars have been recognized overlying, scoured into, or landward of, six of the Lazeart sand bodies.

2. The Lazeart sandstones locally contain up to 10 percent fusinite (charcoal) clasts south of this projects study area near Interstate 80 at the Lazeart Mine. This suggests that distributary channels transported debris from the delta plain and coastal swamps out to sea.

However, the occurrence of a dominant longshore drift may have caused the shoreline to prograde.

An important point to note is that the morphology of a delta front may be drastically different from that of its plain (Elliott, 1981). For instance, the Rhone Delta front is wave-dominated while its plain is fluvial-dominated. The reason for such a difference lies in the delta front's ability to shield the interior plain from wave interactions. The Lazeart wave-dominated system was likely similar to the Rhone. The

Lazeart Member, representing a deltaic front, contains variable trough to hummocky cross-beds that indicate a wave-influenced environment (Figures 14). Herringbone cross-beds are rare, but are an indication of local tidal influence on the delta front. The coal-bearing Adaville Formation, representing the delta plain facies, tends to appear fluvially-dominated with migrating distributary channels (Lawrence, 1992).

The Lazeart wave-dominated system was most likely a deltaic complex throughout most of its history (Lawrence, 1984). However, it is also probably similar to the Dunvegan river- and wave-dominated depositional system (Bhattacharya and Walker 1991). It is a complex three-dimensional progradational system that transformed into other depositional systems due to physical or chemical changes affecting the system's morphologic framework. Observations gathered from this project suggest a wave-dominated setting. However, the scale of my project is not large enough to dispute any published observations within the Adaville Formation or the stratigraphically lower exposures of its Lazeart Member.

Models

Geologists produce and use models to visually and mathematically investigate depositional systems. This study concentrates on prograding deltaic systems, specifically the Lazeart wave-dominated deltaic system. Deltaic systems are extremely complex and their morphologic characteristics often change through time. Models are a useful tool and an important addition to thorough fieldwork. They physically and chemically represent depositional systems and allow geologists to test various hypotheses. Models also provide geologists an opportunity to compare and contrast similar depositional environments. Mathematical modeling of basin analysis can give insight into sediment accumulation, rate of progradation, the evolution of fluid pressure, zonation of slope deposits into time-stratigraphic units, and motivation for basinal subsidence (Horowitz, 1976).

Modern analogs of wave-dominated deltas are the Nile, Rhone, and the Sao Francisco (Figure 46). The Lazeart deltaic system's morphologic characteristics indicate a wave- dominated history. The identification of distributary channels as the dominant sediment source and a linear, virtually north/south, delta front are typical traits of a wave-dominated deltaic system. Lawrence's (1982) depositional model graphically represents the Lazeart wave-dominated deltaic system (Figure 47).

Similar Late Cretaceous wave-dominated deltas also exist in the stratigraphic record. Weise (1980) characterized and modeled the Upper Cretaceous wave-dominated delta system of the San Miguel Formation in southwest Texas. Bhattacharya and Walker's (1991) research on the Upper Cretaceous Dunvegan Formation in northwestern Alberta revealed a complex depositional history. The Dunvegan Formation displays a

stratigraphic series of different transition zone environments. The Adaville-Lazeart-Hilliard depositional series appears to have been dominated by wave action throughout most of its history. However, it is possible that the Lazeart wave-dominated system morphology changed through time. Varying basinal forces may have altered the deltaic regime into a strandplain or barrier island chain.

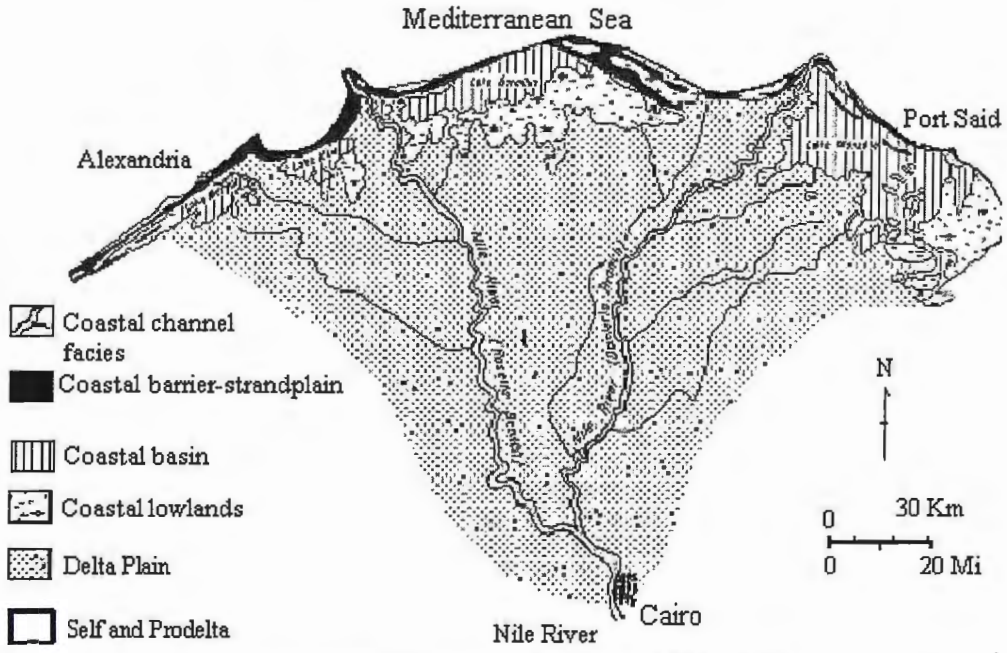

Figure 46. Depositional environments of the wave-dominated Nile delta system, Egypt. (From Fisher et. al., 1969).

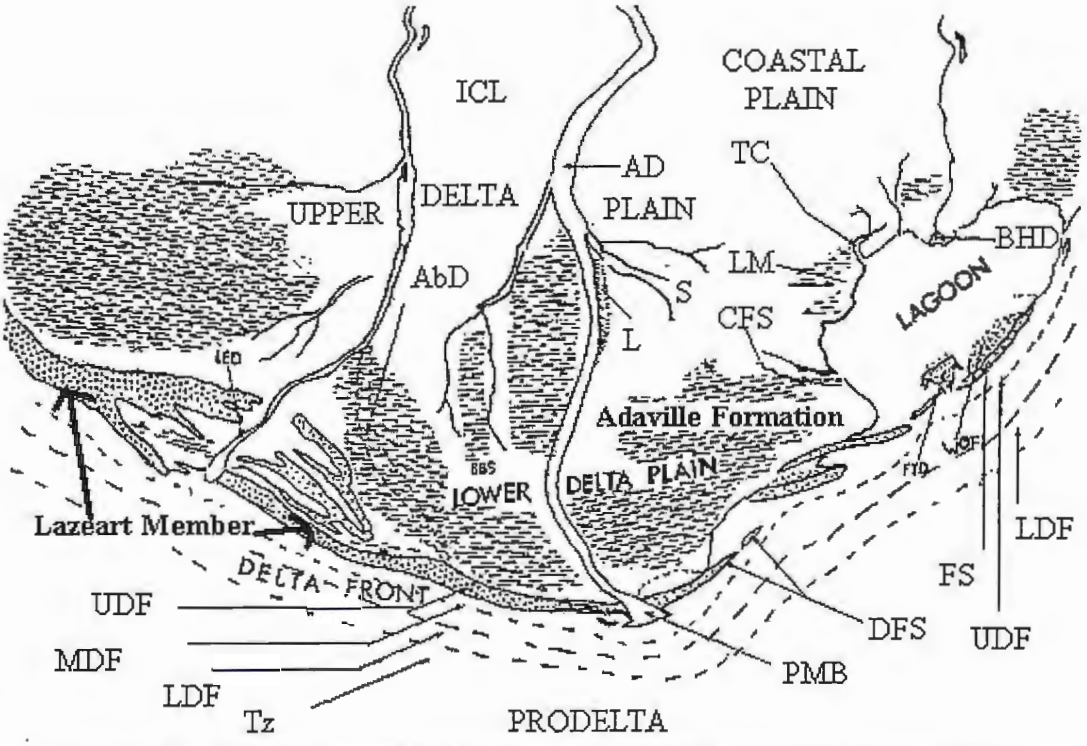

Figure 47. Possible model for the Lazeart-Adaville wave-dominated deltaic system. The illustration shows various stages of construction and abandonment. Not all subenvironments shown existed within the delta at one time. Sub environments are indicated by initials: LDF = lower delta front, MDF = middle delta front, UDF = upper delta front, Tz = transition zone, PMB = proximal mouth bar, DFS = delta flank spits and bars, LED = low energy distributary, AbD = abandoned distributary, BBS = back beach swamp, L = levee, S = splay, AD = active distirbutary, ICL = interchannel lowlands, LM = lower marsh, CFS = channel form slough, TC = tidal channel, BHD = bay head delta. North is to the right of the page. (From Lawrence, 1982, p. 36).

CONCLUSIONS

Petrography

1. The average QmFLt index for sandstones within the Adaville Formation is 70:10: 20, classifying them as feldspathic sublitharenites and feldspathic litharenites.

2. The average QmFLt index for sandstones of the Lazeart Member of the Adaville Formation is 58:10:32, classifying them as feldspathic lithic arenites and feldspathic sublitharenites.

3. The high percentage of dark chert fragments gives the Lazeart sandstones a "salt and pepper" appearance.

4. The Adaville and Lazeart sandstones were lithified by carbonate cement, quartz cement, clay cement, a matrix combination of detrital and authigenic clays, and various combinations of these. The dominant bonding material is a matrix combination of detrital and authigenic clays consisting of illite, smectite, kaolinite, and vermicular kaolinite.

5. Porosity in the Lazeart Member ranges from 11.8 to 23.8 percent (average 17.9 percent). Porosity is absent when the rock is carbonate-cemented. Porosity within sandstones of the Adaville Formation ranges from 6 to 17.2 percent (average 10.5 percent).

6. Vermicular kaolinite and quartz cement have resulted in a decrease in the porosity of the Lazeart sandstones.

7. Thin section, SEM, and EDS verified the altering of K-feldspar to kaolinite and the presence of quartz overgrowths. As quartz overgrowths increase in volume, the amount of feldspar typically decreases. This may be in part diagenetic due to the dissolution of feldspar, with the silica becoming available for cementation.

Provenance

1. The presence of both euhedral and rounded zircon grains indicates multiple source areas, including a recycled sedimentary source and a plutonic source.

2. Chert, siltstone, and rounded zircon grains within the Lazeart Member were recycled from Paleozoic sedimentary units thrust upward and eastward by the

Absaroka and older faults. The Rex Member of the Permian Phosphoria Formation was the likely source for much of the chert within the Lazeart.

3. Euhedral zircons, feldspars, metamorphic fragments, and unstable heavy minerals within the Lazeart Member most likely came from portions of the Idaho batholith.

Paleocurrents

1. Paleocurrent analysis reveals both bimodal and polymodal current directions.

2. A southeastward trend is dominant.

3. A crude bimodality is evident in the first and third Lazeart sandstone bodies. The modes are close to 90°apart, suggestive of currents moving both southeastward (offshore movement of sediment down the delta front) and north-northeastward (wave generated longshore drift parallel to the shoreline). These data fit the wave-dominated delta model for deposition of the Lazeart Member of the Adaville Formation.

4. Uncommon herringbone cross-beds provide evidence of a local tidal influence.

General

1. The sandstone bodies of the Lazeart Member of the Adaville Formation in the vicinity of Kemmerer, Wyoming, fit the proposed model of deposition on the delta front portion of a wave-dominated delta. The cyclicity of the sandstone bodies and shale units is the result of repeated minor marine transgressions and regressions, with the delta progradations southeastward during marine regressions.

2. The lower part of the Adaville Formation that overlies the Lazeart Member contains economic coal seams. These were deposited in organic rich swamps located on the lower delta plain of the Lazeart wave-dominated deltaic complex. Fossils contained within the formation are compatible with marine and brackish water environments of a marine-continental interface.

REFERENCES

Armstrong, F.C, and Oriel, S.S., 1965, Tectonic development of Idaho-Wyoming thrust belt: American Association of Petroleum Geologists Bulletin, v. 49, no. 3, p. 1847-1866.

Beaumont, C., 1981, Foreland basins: Royal Astronomical Society Geophysics Journal, v. 65, p. 291-305

Bhattacharya, J., and Walker, G., 1991, River- and wave-dominated depositional systems of the Upper Cretaceous Dunvegan Formation, northwestern Alberta: Bulletin of Canadian Petroleum Geology, v. 39, no. 2, p. 165-191.

Bickford, M.E., Chase, R.B., Nelson, B.K., Shuster, R.D., and Arruda, E.C., 1981, U-Pb studies of zircon cores and overgrowths, and monzonite: implications for age and petrogenesis of the northeastern Idaho batholith: Journal of Geology, v. 89, p. 433-457.

Bradley, W.H., 1964, Geology of the Green River Formation and associated Eocene rocks in southwestern Wyoming and adjacent parts of Colorado and Utah: U.S. Geological Survey Professional Paper 496-A, p. A 1-A 86.

Breithaupt, B.H., 1990, Early Tertiary fossils and environments of Wyoming Jackson to Fossil Butte National Monument: Geologic Society of Wyoming public circular, 29, p. 57-72.

Carr, T.R., and Paull, R.K., 1983, Early Triassic stratigraphy and paleogeography of the Cordilleran miogeocline, in Reynolds, M.W., and Dolly, E.D., (eds.) Rocky Mountain Paleogeography Symposium 2: Society of Economic Paleontologists and Mineralogists, p. 39-55.

Cobban, W.A., and Reedside, 1962, Correlation of the Cretaceous formations of the western interior of the United States: Geological Society of America Bulletin, v.63, p. 1011-1044.

Coleman, J.M., 1976, Deltas: Processes of deposition and models for exploration: Champaign, Continuing Education Publication Company, Inc., 102 p.

Coleman, J.M., and Wright, L.D., 1975, Modern river deltas: Variability of processes and sand bodies: in Morgan, J.P., (ed.), Deltas, Models for Exploration: Houston Geological Society, p. 99-149.

Coogan, J.C., and Royse, F, 1990, Overview of recent developments in Thrust Belt interpretation: in Roberts, S. (ed.), Geologic field tours of western Wyoming and parts of adjacent Idaho, Montana, and Utah: Geologic Survey of Wyoming, cir. 29, p. 89-127.

Dickinson, W.R., Beard L.S, Brakenridge G.R., Erfavec, J.L., Ferguson, R.C, Inman K.F., Knepp R.A., Lindberg F.A., and Ryberg, P.T., 1983, Provenance of North American Phanerozoic sandstones in relation to tectonic setting: Geological Society of America Bulletin, v. 94, p. 222-235.

Dutton, S.P., 1993, Influence of provenance and burial history on diagenesis of Lower Cretaceous Frontier Formation sandstones, Green River Basin, Wyoming: Journal of Sedimentary Petrology, v. 63, no. 4, p. 665-677.

Elliott, T., 1981, Deltas: in Reading H.G., ed., Sedimentary Environments and Facies: New York, Blackwell Scientific Publications, p. 97-142.

Elliott, T., 1981, Clastic shorelines: in Reading H.G., (ed.), Sedimentary environments and facies: New York, Blackwell Scientific Publications, p. 143-175.

Galloway, W.E., 1975, Process framework for describing the morphologic and stratigraphic evolution of deltaic depositional systems: in Broussard, ed., Deltas: Models for Exploration: Houston Geological Society, p. 87-98.

Gazin, C.L., 1962, A further study of the lower Eocene mammalian faunas of southwestern Wyoming: Smithsonian Miscellaneous Collections, v. 117, no. 18, 82 p.

Goetzmann, W. H., 1966, Exploration and empire: The explorer and the scientist in the winning of the American west: New York, p. 105-530.

Grande, L., 1984, Paleontology of the Green River Formation, with a review of the fish fauna: Geologic Survey of Wyoming Bulletin, v. 63, 333 p.

Feo-Codecido, G., 1956, Heavy mineral techniques and their application to Venezuelan stratigraphy: American Association of Petroleum Geologists Bulletin, v. 40, p. 984-1000.

Fisher, W.L., Brown, L.F., Scott, A.J., and McGowen, J.H., 1969, Delta systems in exploration for oil and gas: Bureau of Economic Geology, University of Texas, Austin, 78p.

Haq, B. U., Hardenbol, J. and Vail, P.R., 1987, Chronology of fluctuation sea levels since the Triassic: Science, v. 235, p. 1156-1166.

Hayes, M.D., 1975, Morphology of sand accumulaion in estuaries: in Cronin, L.E. (ed.), Estuarine Research, v. 2, p. 3-22.

Heward, A.P, 1981, A review of wave-dominated clastic shoreline deposits: Earth-Science Reviews, v. 17, p. 223-276.

Horowitz, D.H., 1976, Mathematical modeling of sediment accumulations in prograding deltaic systems: in Merriam, D.F. (ed.), Quantitative Techniques for the Analysis of Sediments, IX International Sedimentologic Congress, Nice, France, p. 105-120.

Hubert, J.F., 1962, A zircon-tourmaline-rutile maturity index and the interdependence of the composition of heavy mineral assemblages with the gross composition and texture of sandstones: Journal of Sedimentary Petrology, v. 32, p. 440- 450.

Hyndman, D.W., 1984, A petrographic and chemical section through the northern Idaho batholith: The Journal of Geology, v. 92, p. 102.

Jordan, T.E., and Douglass, R.C., 1980, Paleogeography and structural development of the late Pennsylvanian to early Permian Oquirrh Basin, northwestern Utah: in Pouch, T.D., and Magathan, E.R.(eds.): Rocky Mountain Paleogeography Symposium 1: Society of Economic Paleonotologists and Mineralogists, p. 279-340.

Jordan T.E., 1981, Thrust loads and foreland basin evolution, Cretaceous western United States: America Assoc. of Petroleum Geologists Bulletin, v. 65, p. 2506-2520.

Kauffman, E.G., 1976, Cretaceous marine cycles of the western interior: The Mountain Geologist, v. 6, no. 4, 227-245.

Lamerson P.R., 1982, The Fossil Basin and its relationship to the Absaroka thrust fault system; in Powers, R.B., (ed.), Geologic Studies of the Cordilleran thrust belt: Rocky Mountain Association of Geologists, Symposium, Denver, Colo., 1982, v. 1, p. 279-340.

Lawrence, D.T, 1982, Influence of transgressive-regressive pulses on coal-bearing strata of the Upper Cretaceous Adaville Formation, southwestern Wyoming: Utah Geological and Mineral Survey Bulletin 118, p. 32-48.

Lawrence, D.T., 1984, Patterns and dynamics of Late Cretaceous marginal marine sedimentation: Overthrust Belt, southwestern Wyoming [Ph.D. thesis]: New Haven, Connecticut, Yale University, 488 p.

Lawrence, D. T., 1992, Primary controls on total reserves, thickness, geometry, and distribution of coal seams: Upper Cretaceous Adaville Formation, southwestern Wyoming: Geologic Society of America Special Paper 267, p. 69-98.

Lush, A.P., McGrew, A.J., Snoke, A.W., 1988, Allochthonous Archean basement in the northern East Humbolt Range, Nevada: Geology, v. 16, p. 349-353.

M'Gonigle, J.W., and Dover, J.H., 1992, Geologic map of the Kemmerer 30′ × 60′ quadrangle, Lincoln, Uinta, and Sweetwater counties, Wyoming: U.S. Geological Survey, Miscellaneous Investigation Series Map I-2079.

Miller, F.X., 1977, Biostratigraphic correlation of the Mesaverde Group in southwestern Wyoming and northwestern Colorado: Rocky Mountain Association of Geologists 1977 Symposium Volume, p. 117 – 137.

Moore, D.M. and Reynolds R.C., 1997, X-Ray diffraction and the identification and analysis of clay mineral: 2nd ed., Oxford, Oxford University Press, 378 p.

Morgan, J.P., 1970, Depositional processes and products in the deltaic environment: in Morgan, J.P., (ed.), Deltaic Sedimentation; Modern and Ancient: Society of Economic Paleontologists and Mineralogist Special Publication 15, p. 31-47.

Nichols, D.J., 1979, Application of palynology of stratigraphic and structural interpretations in the thrust belt of Wyoming and Utah: Wyoming Geologic Survey Public Information Circular 10, p. 21.

Nichols, D.J., and Jacobson, S.R., 1982, Cretaceous biostratigraphy in the Wyoming thrust belt: Mountain Geologist, v. 19, p. 73-78.

Pettijohn, F.J., Potter, P.E., and Siever, R., 1987, Sand and Sandstone: 2nd ed., New York, Springer-Verlag, 553 p.

Phillips, F.C., 1954, Use of stereographic projection in structural geology: London, Edward Arnold Publishers, p. 29-31.

Pivnik, D.A., 1990, Thrust-generated fan-delta deposition: Little Muddy Creek Conglomerate, SW, Wyoming: Journal of Sedimentary Petrology, vol. 60, no. 4, p. 489-503.

Potter, P.E., and Pettijohn, F.J., 1977, Paleocurrents and Basin Analysis: 2nd ed., New York, Springer-Verlag, 390 p.

Potter, P.E., and Pryor, W.A., 1961, Dispersal centers at Paleozoic and later clastics of the upper Mississippi valley and adjacent areas: Geologic Society of America Bulletin, v. 72, p. 1195-1250.

Rogers, R.R., 1998, Sequence analysis of the Upper Cretaceous Two Medicine and Judith River Formations, Montana: Nonmarine response to the Claggett and Bearpaw marine cycles: Journal of Sedimentary Research, vol. 68, no. 4, p. 615-631.

Rubey, W.W., Oriel, S.S., and Tracey J.I., 1975, Geology of the Sage and Kemmerer 15-Minute Quadrangles, Lincoln County, Wyoming: U.S. Geologic Survey Professional Paper 855, 18 p.

Ryu, I.C., and Niem, A.R., 1999, Sandstone diagenesis, reservoir potential, and sequence stratigraphy of the Eocene Tyee Basin, Oregon: Journal of Sedimentary Research, v. 69, no. 2, p. 384-393.

Scholle, P. A., 1979, A color illustrated guide to constituents, textures, cements, and porosities of sandstones and associated rocks: American Association of Petroleum Geologist Memoir, no. 28, 201 p.

Speed, R.C, and Sleep, N.H., 1982, Antler orogeny and foreland basin: a model: Geological Society of America Bulletin, v. 93, p. 815-828.

Surdam, R.C., and Wolfbauer, C.A., 1975, Green River Formation, Wyoming: A playa lake complex: Geologic Society of America Bulletin, v. 86, p. 335-345.

Tweto, O., 1975, Laramide (Late Cretaceous-Early Tertiary) Orogeny in the southern Rocky Mountains: Geological Society of America Memoir 144, p. 1-44.

Veatch, A.C., 1907, Geography and geology of a portion of Southwestern Wyoming: U.S. Geologic Survey Professional Paper 56, 166 p.

Vital, H., Stattegger, K., and Garbe-Schonberg, C.D., 1999, Composition and trace-element geochemistry of detrital clay and heavy mineral suites of the lowermost Amazon River: A Provenance study: Journal of Sedimentary Research, vol. 69, no. 3, p. 563-575.

Weimer, R.J., 1970, Rates of deltaic sedimentation and intrabasin deformation, Upper Cretaceous of Rocky Mountain Region: in Morgan, J.P., ed., Deltaic sedimentation; modern and ancient: Society of Economic Paleontologists and Mineralogist Special Publication 15, p. 270-292.

Weimer, R.J., 1960, Upper Cretaceous stratigraphy, Rocky Mountain area: American Association of Petroleum Geologists Bulletin, v. 44, no. 1, p. 1-20.

Weise, B.R., 1980, Wave-dominated delta systems of the Upper Cretaceous San Miguel Formation, Maverick Basin, south Texas: Texas Bureau of Economic Geology Report of Investigation, no. 107, p. 1-39.

Young, S.W., 1976, Petrographic textures of detrital polygonal quartz as an aid to interpreting crystalline source rocks: Journal of Sedimentary Petrology v. 50, p. 595-603.